Submitted to Astrophys. J.

Neutrino astronomy with the MACRO detector

The MACRO Collaboration

M. Ambrosio[12], R. Antolini[7], G. Auriemma[14,a], D. Bakari[2,17], A. Baldini[13], G. C. Barbarino[12], B. C. Barish[4], G. Battistoni[6,b], R. Bellotti[1], C. Bemporad[13], P. Bernardini[10], H. Bilokon[6], V. Bisi[16], C. Bloise[6], C. Bower[8], M. Brigida[1], S. Bussino[18], F. Cafagna[1], M. Calicchio[1], D. Campana[12], M. Carboni[6], S. Cecchini[2,c], F. Cei[13], V. Chiarella[6], B. C. Choudhary[4], S. Coutu[11,m], G. De Cataldo[1], H. Dekhissi[2,17], C. De Marzo[1], I. De Mitri[10], J. Derkaoui[2,17], M. De Vincenzi[18], A. Di Credico[7], O. Erriquez[1], C. Favuzzi[1], C. Forti[6], P. Fusco[1], G. Giacomelli[2], G. Giannini[13,e], N. Giglietto[1], M. Giorgini[2], M. Grassi[13], L. Gray[7], A. Grillo[7], F. Guarino[12], C. Gustavino[7], A. Habig[3], K. Hanson[11], R. Heinz[8], E. Iarocci[6,f], E. Katsavounidis[4], I. Katsavounidis[4], E. Kearns[3], H. Kim[4], S. Kyriazopoulou[4], E. Lamanna[14,o], C. Lane[5], D. S. Levin[11], P. Lipari[14], N. P. Longley[4,i], M. J. Longo[11], F. Loparco[1], F. Maaroufi[2,17], G. Mancarella[10], G. Mandrioli[2], S. Manzoor[2,n], A. Margiotta[2], A. Marini[6], D. Martello[10], A. Marzari-Chiesa[16], M. N. Mazziotta[1], D. G. Michael[4], S. Mikheyev[4,7,g], L. Miller[8,p], P. Monacelli[9], T. Montaruli[1,*], M. Monteno[16], S. Mufson[8], J. Musser[8], D. Nicolò [13,d], R. Nolty[4], C. Okada[3], C. Orth[3], G. Osteria[12], M. Ouchrif[2,17], O. Palamara[7], V. Patera[6,f], L. Patrizii[2], R. Pazzi[13], C. W. Peck[4], L. Perrone[10], S. Petrera[9], P. Pistilli[18], V. Popa[2,h], A. Rainò [1], J. Reynoldson[7], F. Ronga[6], C. Satriano[14,a], L. Satta[6,f], E. Scapparone[7], K. Scholberg[3], A. Sciubba[6,f], P. Serra[2], M. Sioli[2], M. Sitta[16], P. Spinelli[1], M. Spinetti[6], M. Spurio[2], R. Steinberg[5], J. L. Stone[3], L. R. Sulak[3], A. Surdo[10], G. Tarlè [11], V. Togo[2], M. Vakili[15], E. Vilela[2], C. W. Walter[3,4] and R. Webb[15].

1. Dipartimento di Fisica dell'Università di Bari and INFN, 70126 Bari, Italy
2. Dipartimento di Fisica dell'Università di Bologna and INFN, 40126 Bologna, Italy
3. Physics Department, Boston University, Boston, MA 02215, USA
4. California Institute of Technology, Pasadena, CA 91125, USA
5. Department of Physics, Drexel University, Philadelphia, PA 19104, USA
6. Laboratori Nazionali di Frascati dell'INFN, 00044 Frascati (Roma), Italy
7. Laboratori Nazionali del Gran Sasso dell'INFN, 67010 Assergi (L'Aquila), Italy
8. Depts. of Physics and of Astronomy, Indiana University, Bloomington, IN 47405, USA
9. Dipartimento di Fisica dell'Università dell'Aquila and INFN, 67100 L'Aquila, Italy
10. Dipartimento di Fisica dell'Università di Lecce and INFN, 73100 Lecce, Italy
11. Department of Physics, University of Michigan, Ann Arbor, MI 48109, USA
12. Dipartimento di Fisica dell'Università di Napoli and INFN, 80125 Napoli, Italy
13. Dipartimento di Fisica dell'Università di Pisa and INFN, 56010 Pisa, Italy
14. Dipartimento di Fisica dell'Università di Roma "La Sapienza" and INFN, 00185 Roma, Italy
15. Physics Department, Texas A&M University, College Station, TX 77843, USA
16. Dipartimento di Fisica Sperimentale dell'Università di Torino and INFN, 10125 Torino, Italy

17. L.P.T.P., Faculty of Sciences, University Mohamed I, B.P. 524 Oujda, Morocco
18. Dipartimento di Fisica dell'Università di Roma Tre and INFN Sezione Roma Tre, 00146 Roma, Italy
a Also Università della Basilicata, 85100 Potenza, Italy
b Also INFN Milano, 20133 Milano, Italy
c Also Istituto TESRE/CNR, 40129 Bologna, Italy
d Also Scuola Normale Superiore di Pisa, 56010 Pisa, Italy
e Also Università di Trieste and INFN, 34100 Trieste, Italy
f Also Dipartimento di Energetica, Università di Roma, 00185 Roma, Italy
g Also Institute for Nuclear Research, Russian Academy of Science, 117312 Moscow, Russia
h Also Institute for Space Sciences, 76900 Bucharest, Romania
i The Colorado College, Colorado Springs, CO 80903, USA
m Also Department of Physics, Pennsylvania State University, University Park, PA 16801, USA
n Also RPD, PINSTECH, P.O. Nilore, Islamabad, Pakistan
o Also Dipartimento di Fisica dell'Università della Calabria, Rende (Cosenza), Italy
p Also Department of Physics, James Madison University, Harrisonburg, VA 22807, USA
∗ Corresponding author, e-mail: montaruli@ba.infn.it

ABSTRACT

High energy gamma ray astronomy is now a well established field and several sources have been discovered in the region from a few GeV up to several TeV. If sources involving hadronic processes exist, the production of photons would be accompanied by neutrinos too. Other possible neutrino sources could be related to the annihilation of WIMPs at the center of galaxies with black holes.

We present the results of a search for point-like sources using 1100 upward-going muons produced by neutrino interactions in the rock below and inside the MACRO detector in the underground Gran Sasso Laboratory. These data show no evidence for a possible neutrino point-like source or for possible correlations between gamma ray bursts and neutrinos. They have been used to set flux upper limits for candidate point-like sources which are in the range $10^{-14} - 10^{-15}$ cm^{-2} s^{-1}.

Subject headings: neutrinos, upward-going muons

1. Motivations for neutrino astronomy

The origin of cosmic rays is still largely an open question. The cosmic ray spectrum extends up to 10^{20} eV and the nature of the mechanisms capable of explaining such high energies is still unknown. Due to magnetic fields, charged cosmic particles are deflected from their original direction, hence the information on the position of their source is lost. On the other hand, protons of energies $\gtrsim 10^7$ TeV and neutral particles, such as photons and neutrinos, point back to their sources since they are not deflected by magnetic fields. However, the universe should become opaque to protons with energies above $\sim 5 \cdot 10^{19}$ eV at distances of ~ 30 Mpc due to photo-pion production when

they interact with the Cosmic Microwave Radiation (CMBR) (1). Photons are currently the main observation channel of our universe and the field of gamma-ray astronomy is now well established.

The idea of using neutrinos as probes of the deep universe was introduced in the sixties. Already in those years the first calculations on the diffuse neutrino flux from interactions of cosmic rays in the Galaxy (2) and of high energy neutrinos from the Crab (3) were performed.

Neutrinos are weakly interacting particles and are therefore much less absorbed than gamma rays, which are not only absorbed during their propagation, but can even be absorbed by the source producing them. Neutrinos can bring information on the deep interior of sources and on the far Universe. Several examples of detection of cosmic neutrinos already exist: solar neutrinos (from 0.1 MeV up to around 10 MeV), first detected by Homestake (4), and neutrinos from SN1987A (from $\sim$ 10 MeV up to $\sim$ 50 MeV) detected by Kamiokande and IMB (5; 6). Nevertheless, neutrinos of astrophysical origin with energies larger than 100 MeV have not yet been observed. This observation would open the new field of high energy neutrino astronomy complementary to gamma ray astronomy. Moreover, an important hint on the existence of neutrino astronomy would come from the detection of photons of energies above 100 TeV. Such energies, in fact, cannot be explained by electron energy loss mechanisms (e.g. synchrotron radiation, bremsstrahlung and inverse Compton scattering) because electron acceleration is limited by the intense synchrotron radiation produced in the ambient magnetic fields. Therefore, alternate acceleration mechanisms which involve neutrinos are required.

Satellites, ground based imaging Cherenkov telescopes and extensive air shower arrays are currently investigating the universe, cosmic ray sources and acceleration mechanisms using photons as probes (7). Current Space experiments typically work in the energy range up to about 30 GeV and ground-based terrestrial experiments have typical threshold energies of about 250 GeV. Ground based experiments have larger surfaces and longer time exposures than space experiments, therefore they can observe higher energies where fluxes are low. Nevertheless, they are limited at low energies by the large background due to gamma rays produced in the electromagnetic cascades induced by cosmic ray interactions in the atmosphere.

The EGRET detector on board the Compton Gamma Ray Observatory (CGRO) satellite has thus far furnished the largest amount of information on sources up to $\sim$ 30 GeV. The recent third EGRET catalogue (8), covering the observations made from 1991 to 1995, contains 271 sources observed with energies greater than 100 MeV. Between them, there are 5 pulsars, one probable radio galaxy (Cen A), 66 high-confidence identifications of blazars (BL Lac objects and radio quasars), 27 lower-confidence potential blazar identifications and a large number of identified supernova remnants (SNRs), and also 170 sources not yet identified firmly with known objects.

Satellite based detectors are providing observations on γ-ray bursts (GRBs) capable of solving the mystery concerning their nature. The BATSE experiment (9) on CGRO satellite has now detected more than 2500 γ-ray bursts and the Italian-Dutch *Beppo*SAX satellite (10) is providing breakthroughs thanks to the precise measurement (the error box radius is at the level of 4') of the

position of the bursts. Ground based experiments are looking for emissions above the TeV from GRBs: recently the Milagrito detector has found a correlation with the BATSE GRB970417a with chance probability 1.5×10^{-3} (11).

Cherenkov telescopes at ground level such as the Whipple observatory, HEGRA, Cangaroo and University of Durham Mark 6 telescopes, have so far detected 8 sources emitting γ-rays well above 300 GeV: the supernova remnants Crab (12), Vela Pulsar (at a distance of only $\sim$ 500 pc)(13), SN1006 (14), the extra-galactic BL Lac objects (highly variable active galactic nuclei) Mkn 421 ($z = 0.031$)(15; 16), Mkn 501 ($z < 0.034$) (17), PKS2155-304 ($z = 0.116$) (18), and the pulsars PSR1706-44 (19), PSR1259-63 (20). The Whipple group detected the first source, the Crab supernova remnant (12). The Crab is considered now as a standard candle for high energy gamma ray astronomy due to its gamma ray steady emission.

The number of sources detected so far by ground based experiments is much smaller than the number of sources detected by EGRET. One of the possible explanations is that high energy gamma rays are absorbed: TeV γ-rays suffer absorption through pair production in intergalactic space on infrared light, PeV γs on the CMBR and EeV γs on radio-waves. This can even explain why the only BL Lac objects observed till now are also the nearest ones.

The discovery of TeV gamma rays emitted from the 8 sources quoted above shows the possibility of production from π^o decay and the possible existence of beam dump sources (see Sec. 2) producing high energy neutrinos. Nevertheless, "a few TeV" are energies not high enough to exclude a synchrotron radiation production mechanism. It could be completely excluded only for sources of energies above 100 TeV, but up to now, no source emitting at such energies has been discovered. There were some claims in the past, particularly about Cygnus X3, but they have not been confirmed (21).

A different kind of neutrino production from astrophysical sources has been suggested by Gondolo and Silk (22). If cold dark matter exists in the Galactic Center, it can be accreted by the black hole which probably is there. The cold dark matter is redistributed by the black hole into a cusp, which they call "central spike". If dark matter is made of neutral particles that can annihilate, such as the supersymmetric neutralino, the annihilation rate in the spike is strongly increased as it depends on the square of the matter density. Neutrinos can escape and produce relevant fluxes. For the neutralino, the fluxes are very high in the case of the presence of a central spike at the level of $10^{-15} \div 10^{-14}$ cm^{-2} s^{-1} for $m_\chi \gtrsim 50$ GeV.

During the '70s and '80s the first generation underground detectors of surface $\sim$ 100 m^2 have been measuring neutrinos. Those detectors were aimed at detecting proton decay for which atmospheric neutrinos were considered a background. Nevertheless, neutrinos were soon considered as an interesting signal themselves and results on searches for astrophysical sources of neutrinos were made. Previous results on the search for point-like sources have been published by the Kolar Gold Field experiment (23) and by the water Cherenkov detectors IMB (24) and Kamiokande (25). Other experiments (Baksan (26) and AMANDA (27)) have presented preliminary results

at conferences. MACRO has been detecting muon neutrinos since 1989 while it was still under construction. We present here the results of the search for astrophysical neutrino sources with MACRO during the period March 1989 - September 1999.

2. Neutrino astronomy

Astrophysical neutrinos can be produced in the interactions of protons accelerated by compact sources with a target around the source (gas of matter or photons). This is the most plausible model for a neutrino source, the so called "beam dump model" (28; 29). The acceleration process requires the presence of a strong magnetic field with sufficient local gas to act as a beam dump. The column density of the gas in the source is assumed to be larger than the nuclear depth ($x_N \sim 70$ g/cm^2), but smaller than the neutrino absorption depth due mainly to νN interactions ($x_\nu \sim 3 \cdot 10^{12} \cdot 100$ GeV$/E_\nu$ g/cm^2 and $x_{\bar{\nu}} \sim 6 \cdot 10^{12} \cdot 100$ GeV$/E_{\bar{\nu}}$ g/cm^2 (28)). The chain of reactions is:

$$\begin{array}{lllll} p + N(\gamma) \rightarrow \pi^0 & + & \pi^\pm + ... & & \\ \quad \searrow \gamma + \gamma & & \searrow \mu^\pm + \nu_\mu(\bar{\nu}_\mu) & & \\ & & & \searrow e^+ + \nu_e + \bar{\nu}_\mu \;\; (e^- + \bar{\nu}_e + \nu_\mu)\,. & \end{array} \tag{1}$$

Neutral pions produce the observed photons; from the same chain it is expected the production of charged pions and kaons which can decay producing neutrinos and muons. Moreover, muons decay too. The result are neutrinos and antineutrinos of electron and muon flavors. Neglecting the photon absorption effect, which is subject to very large uncertainties, the neutrino flux have at least the same spectral shape and intensity with respect to the gamma ray flux; hence very low neutrino event rates are expected due to the small neutrino cross section. The presence of $\gtrsim 100$ TeV gamma ray sources should guarantee the existence of neutrino sources, but no reliable information could be drawn on neutrino fluxes from gamma ray ones because they are subject to non negligible absorption.

Cosmic accelerators produce a power law spectrum:

$$\frac{d\phi}{dE} \propto E^{-(\gamma+1)} \tag{2}$$

where $\gamma \sim 1 + \varepsilon$, with ε a small number. The first order Fermi acceleration mechanism in strong shock waves has the attractive feature of resulting in this kind of power spectrum (30) and it predicts a spectral index $\gamma \sim 1$. The primary cosmic ray spectrum is thought to be steeper than the one resulting from a cosmic accelerator because of the energy dependence of the cosmic ray diffusion out of the Galaxy, as explained in (29).

Primary cosmic rays interact with the nuclei in the atmosphere and produce cascades from which atmospheric neutrinos of muon and electron flavor originate from the decays of pions, kaons and muons. Up to now, only atmospheric neutrinos with energies above 100 MeV have been detected by underground detectors. If all the parent mesons of atmospheric neutrinos decay the

neutrino spectrum follows the spectrum of the parent particles ($(\frac{d\phi_\nu}{dE})_{atm} \propto E^{-2.7}$ for $E_\nu \lesssim 10$ GeV). For higher energies, since the path length in the atmosphere is not large enough to allow the decay of all pions and kaons, interactions of mesons begin to dominate and the atmospheric neutrino spectrum becomes steeper ($(\frac{d\phi_\nu}{dE})_{atm} \propto E^{-3.7}$ for $E_\nu \gtrsim 100$ GeV) due to the change of the spectral index of the meson spectra. These neutrinos originating in the Earth atmosphere are a background for the search for astrophysical neutrinos which, on the other hand, are produced by cosmic rays at their acceleration sites and hence should follow the hard cosmic ray source spectrum of the form:

$$\left(\frac{d\phi_\nu}{dE_\nu}\right)_{source} \propto E^{-(2.0 \div 2.5)} \,. \tag{3}$$

Thus the signal to noise ratio becomes larger at increasing energies, and above some tens of TeV the neutrinos from sources start to dominate.

The search presented here uses only the direction information of the neutrinos. Other searches could maximize the signal to noise ratio using the energy information on the detected particle and looking to the diffuse neutrino events from the whole sky. This was done by the Frejus experiment (31) and some results have been recently presented by the Baikal collaboration (32). Preliminary MACRO results were presented elsewhere (33) and will be the subject of a future paper.

2.1. Candidate sources and expected rates

High energy neutrinos are expected to be emitted from a wide class of possible celestial objects which can be divided into two wide classes: galactic sources and extragalactic sources (29).

Galactic sources are energetic systems, such as binary systems and supernova remnants, in which cosmic rays (CRs) are accelerated and interact with matter (mainly protons). The most interesting sources are SNRs, which are the most likely sources to be observed by a detector of the MACRO size. In such systems, the target is the material of the expanding shell and the accelerating mechanism is originated by the intense magnetic field of the pulsar. There are however possibilities to have neutrino emissions originate by acceleration at the supernova blast waves and therefore neutrino emission even without pulsars. The neutrino emission should be in an active time of up to a few years. Of course the disadvantage of galactic supernovae as neutrino emitters is that their rate is low (of the order of 1/30 years). According to detailed calculations made for several historical supernova (34), the most intense source should be the supernova remnant Vela Pulsar with a rate of upward-going muons induced by neutrinos in the rock surrounding a detector of the order 0.1 ev/yr/1000 m^2 for E_μ >1 GeV. Another model for young SNRs with a pulsar having high magnetic field and short period ($\sim$ 5 ms) is suggested in Ref. (35): for a beaming solid angle of neutrino emission of 1 sr, about 5 events/yr are expected in 1000 m^2 for $E_\nu \geq 100$ GeV after 0.1 yr from an explosion at a distance of 10 kpc.

A different kind of galactic source is suggested in Ref. (22) due to WIMP annihilations in the

core of the Galactic Center. The rates would be very promising, even for detectors like MACRO, being of the order of 1-20 events/yr/1000 m^2.

Possible extragalactic sources are active galactic nuclei and gamma-ray bursters. For these sources the dominant mechanism for producing neutrinos is accelerated protons interacting on ambient photons. Possible alternative mechanisms are the so called Top-Down models (36).

Active galactic nuclei (AGNs), being among the most luminous objects in the Universe with luminosities ranging from 10^{42} to 10^{48} erg/s, have been recognized for a long time as promising possible sources of neutrinos. Present models assume that they consist of a central engine (massive black hole) with an accretion disk and jets (29). Accretion onto the central black hole provides the total power. Two possible sources of high energy neutrino fluxes within AGNs have been suggested. The first is associated with the central engine and the second with the production in jets associated with several blazars (radio-loud AGNs in which the beam intersects the observer line of sight). AGNs could emit neutrinos up to $\sim 10^{10}$ GeV.

Even considering the highest luminosities and the presence of jets, single AGNs are difficult to detect. Jets carry about 10% of the AGN luminosity and AGNs may appear brighter because of the motion of the emitting matter toward the observer (for an observer looking along the jet axis $E_{obs} = \Gamma E_{jet}$ and $L_{obs} = \Gamma^4 L_{jet}$, where Γ is the Lorentz factor). Expected event rates for blazars are of the order of $10^{-2} - 10^{-1}$ /1000 m^2/yr for $\Gamma = 10 - 10^2$ and $E_\nu > 1$ TeV (37).

Stecker *et al.* (38) suggested the possibility to integrate the neutrino flux from single generic AGNs to obtain a diffuse flux from all cosmological AGNs. Various models have been suggested (38; 39) [1] and the event rates in upward-going muons vary between $\sim 10^{-1} - 10$ /1000 m^2/yr for $E_\nu > 1$ TeV.

Gamma Ray Bursters are considered as promising sources of high energy neutrinos. They yield transient events originating beyond the solar system, with typical durations of $10^{-2} \div 10^3$ s. The BATSE (9) experiment has now collected more than 2500 events which appear isotropically distributed. This feature suggests that they are located at cosmological distances. The recent observations by *Beppo*SAX of GRB970228 have allowed the precise measurement of the position which for the first time led to the identification of a fading optical counterpart (40). Immediately after, the direct measurement of the redshift in the optical afterglow at $z = 0.835$ for GRB970508 (41) and other identifications of the distances of GRBs have given support to the cosmological origin hypothesis. These observations make GRBs the most luminous objects observed in our universe with emitted energies $\gtrsim 10^{51}$ erg and a spectrum peaked between 100 keV $\div$ 1 MeV.

One of the most plausible models is the "fireball model", which solves the compactness problem introducing a beamed relativistic motion with $\Gamma \gtrsim 100$ of an expanding fireball (42).

The question of the energy of the engine of GRBs, which is strictly connected to that of

[1] Most of the Szabo and Protheroe (39) models are excluded by the Frejus limit (31).

beaming, is still under discussion. Evidence for beaming are a break and a steepening of the spectrum. They have been found in spectra of some bursts, e.g. GRB980519 and GRB990123; in the case of GRB990123 at $z = 1.6$ for isotropic emission the emitted energy would be the highest ever observed ($2 \cdot 10^{54}$ erg) while if there is a beam the emitted energy would be reduced to $\sim 10^{52}$ erg due to the Lorentz factor.

Several authors have suggested a possible correlation between Gamma Ray Bursters and emissions of high energy neutrinos (43; 44; 45; 46) produced by accelerated protons on photons. Expected rates could be up to 10^6 muon induced events in a 1000 m^2 detector for muon energies above ~ 30 TeV for emissions lasting < 1 s (43). In other scenarios, such as for fireballs, rates are of the order of $\sim 10^{-3}$ upward-going muons in a 1000 m^2-size detector for a burst at a distance of 100 Mpc producing $0.4 \cdot 10^{51}$ erg in 10^{14} eV neutrinos (47). Considering a rate of 10^3 bursts per year over 4π sr, averaging over burst distances and energies, $\sim 2 \cdot 10^{-2}$ upward-going muons are expected in 1000 m^2 per 1 yr for 4π sr (44). It is important to consider that the uncertainty on the Lorentz factor Γ produces high variations in the expected rates: the higher the Γ, the larger the luminosity at the observer ($L_{obs} \sim \Gamma^4 L_{jet}$), but the smaller are the rates of events because the actual photon target density in the fireball is diluted by large Lorentz factors (the fraction of total energy going into pion production in the source and hence into neutrinos varies approximately as Γ^{-4} (48)).

According to Waxman and Bahcall (WB) (47) an energy independent upper bound on diffuse fluxes of neutrinos with $E_\nu \gtrsim 10^{14}$ eV produced by photo-meson or p-p interactions in sources from which protons can escape can be estimated at the level of $E_\nu^2 \phi_\nu < 2 \times 10^{-8}$ GeV cm^{-2} s^{-1} sr^{-1}. This bound relies on the flux measurement of extremely high energy cosmic rays in extensive air showers, which are assumed to be of extragalactic origin. Their limit would exclude most of the present models of neutrino production in AGNs which are commonly normalized to the extragalactic MeV-GeV gamma-ray background. Contrary to WB, Mannheim, Protheroe and Rachen (49) find an energy dependent upper limit which agrees within a factor of 2 with WB in the limited range of $E_\nu \sim 10^{16-18}$ eV, while at other energies the neutrino flux is mainly limited by their contributions to extragalactic gamma-ray background which is at a level of about 2 orders of magnitude higher than the WB limit.

3. The MACRO detector and the data selection

In the range of energies from several GeV to several TeV the neutrinos produced by astrophysical sources can be detected in underground detectors as upward-going muons produced by neutrino charged current (CC) interactions in the rock surrounding the detector. Neutrino events can be discriminated from among the background of atmospheric muons of many orders of magnitude larger ($\sim 5 \cdot 10^5$ at MACRO depth) recognizing that they travel from the bottom to the top of the apparatus after having transversed the Earth. Neutrino detection is experimentally much more difficult than the gamma ray one; because of the low neutrino interaction cross section it requires

very large detectors.

The MACRO detector, shown in Fig. 1 and described in detail in (50) is located in the Hall B of the Gran Sasso underground laboratory at a minimum rock depth of 3150 hg/cm^2 and an average rock depth of 3700 hg/cm^2. The detector, 76.6 m long, 12 m wide and 9.3 m high, is divided longitudinally in six similar supermodules and vertically in a lower part (4.8 m high) and an upper part (4.5 m high).

The active detectors include 14 horizontal and 12 vertical planes of 3 cm wide limited streamer tubes for particle tracking, and liquid scintillation counters for fast timing. In the lower part, the eight inner planes of limited streamer tubes are separated by passive absorbers (iron and rock ~ 50 g cm^{-2}) in order to set a minimum threshold of ~ 1 GeV for vertical muons crossing the detector. The upper part of the detector is an open volume containing electronics and other equipment. The horizontal streamer tube planes are instrumented with external 3 cm pick-up strips at an angle of 26.5° with respect to the streamer tube wires, providing stereo readout of the detector hits. The transit time of particles through the detector is measured by the time of flight technique (T.o.F.) using scintillation counters. The mean time at which signals are observed at the two ends of each counter is measured and the difference in the measured mean time between counters located in different planes gives the T.o.F.. The time resolution of the scintillation counter system is about 500 ps.

In order to achieve the largest reconstruction efficiency for all directions, three algorithms for muon tracking are used in this analysis. The first kind of tracking is for events with aligned hits in at least 4 horizontal planes; the second is for events with at least 2 horizontal planes in coincidence with at least 3 vertical planes; the third is for events having at least 3 vertical planes in coincidence with two scintillation counters (this tracking is useful for almost horizontal tracks).

The angular resolution depends on the wire and strip cluster widths and on the track length. The average errors on the slopes of tracks are 0.14° for the wires and 0.29° for the strips (50). Our pointing capabilities for point-sources has been checked with the observation of the Moon shadowing effect using atmospheric down-going muons (51).

The data used for the upward-going muon search belong to three running periods with different apparatus configurations: 26 events have been detected with the lower half of the first supermodule from March 1989 until November 1991 (about 1/12 of the full acceptance, livetime of 1.38 years, efficiencies included), 55 with the full lower half of the detector (about 60% of the full acceptance) from December 1992 until June 1993 (0.41 years, efficiencies included). Starting from April 1994 the apparatus has been running in the final configuration. From April 1994 until Sep. 1999 we have measured 1000 events with the full detector (4.41 live years, including efficiencies). We also consider events which were measured during periods when the detector acceptance was changing with time due to construction works (19 events during 1992, 0.2 yr).

The selection of upward-going muons using the T.o.F. technique has been described in detail in Ref. (52; 53). The velocity and direction of muons is determined from the T.o.F. between at least

2 scintillation layers combined with the path length of a track reconstructed using the streamers. Taking as a reference the upper counter which measures the time T_1, the time of flight $\Delta T = T_1 - T_2$ is positive if the muon travels downward und it is negative if it travels upwards. Fig. 2 shows the $1/\beta = c\Delta T/L$ (L is the track-length, and c the speed of light) distribution for the entire data set. In this convention, muons going down through the detector have $1/\beta \sim 1$, while muons going upwards have $1/\beta \sim -1$. Several cuts are imposed to remove backgrounds caused by radioactivity in coincidence with muons and multiple muons. The main cut requires that the position of a muon crossing a scintillator agrees within 70 cm (140 cm for slanted tracks with $\cos\theta \leq 0.2$) with the position along the counter determined by the more precise streamer system. Other cuts apply only to events which cross 2 scintillator planes only. These cuts tend to remove high multiplicity events because when more than one track crosses the same scintillator box the reconstructed time of the event is wrong. Events which cross more than 2 scintillator planes (about 50% of the total) have a more reliable time determination thanks to the possibility to evaluate the velocity of the particle from a linear fit of times as a function of the height of the scintillator counters. In this case, the only cut then is on the quality of the fit ($\chi^2 \leq 10$).

Events in the range $-1.25 < 1/\beta < -0.75$ are defined to be upward-going muon events. There are 1100 events which satisfy this definition summed over all running periods. One event is shown in Fig. 3. In order to maximize the acceptance for this search, we do not require a minimum amount of material be crossed by the muon track as was done to select the sample used for the neutrino oscillation analysis (52; 53). Without this requirement we introduce some background due to large angle pions produced by down-going muons (54). We also include events with an interaction vertex inside the lower half of the detector. All of these data can be used for the point-like astrophysical source search since the benefit of a greater exposure for setting flux limits offsets the slight increase of the background and of the systematic error in the acceptance. Moreover, one can notice that for neutrino oscillation studies upward-going muons are mostly signal and background rejection is very critical, while for neutrino astronomy upward-going muons are mostly background due to atmospheric neutrinos and background rejection is less critical.

4. Neutrino signal in upward-going muons

Muon neutrinos are detected as upward-going muons through CC interactions:

$$\nu_\mu(\bar{\nu}_\mu) + N \rightarrow \mu^-(\mu^+) + X\,. \tag{4}$$

The probability that a neutrino (or antineutrino) with energy E_ν interacts in the rock below the detector and gives rise to a muon which crosses the apparatus with energy $E_\mu \geq E_\mu^{th}$ (E_μ^{th} is the energy threshold of the apparatus) is:

$$P_\nu(E_\nu, E_{th}^\mu) = N_A \int_0^{E_\nu} dE_\mu^{'} \frac{d\sigma_\nu}{dE_\mu^{'}}(E_\mu^{'}, E_\nu) \cdot R_{eff}(E_\mu^{'}, E_{th}^\mu) \tag{5}$$

where N_A is Avogadro's number. This probability is a convolution of the ν cross sections and of the muon effective range $R_{eff}(E_\mu, E_\mu^{th})$ described below; the computed probability is shown in Fig. 4 and some values are given in Tab. 1. The trend of the probability at energies $\lesssim 1$ TeV reflects the cross-section linear rise with neutrino energy ($\sigma_\nu \propto E_\nu$) and that of the muon range ($R_{eff} \propto E_\mu$), while at higher energies it reflects the damping effect of the propagator ($\sigma_\nu \propto E_\nu^{0.4}$ for $E_\nu \gtrsim 10^3$ TeV) and the logarithmic rise of the muon range with its energy.

It is relevant to notice that, thanks to the recent HERA measurements (55), our knowledge of the high energy deep inelastic neutrino cross section has improved significantly. There is good agreement between various sets of parton functions which provide confident predictions of the cross-sections up to 10^6 GeV (56). For the calculation of the probability shown in Fig. 4 we have used the CTEQ3-DIS (57) parton function, available in the PDFLIB CERN library (58), which have been considered by Gandhi *et al.* (56) and in good agreement with the more recent CTEQ4-DIS.

The technique of detecting upward-going muons generated in the rock surrounding a detector has the advantage to increase the effective detector mass, which in fact is a convolution of the detector area and of the muon range in the rock. The gain increases with energy: for example, for TeV muons, the range is of the order of 1 km. The effective muon range is given by the probability that a muon with energy E_μ survives with energy above threshold after propagating a distance X:

$$R_{eff}(E_\mu, E_{th}^\mu) = \int_0^\infty dX\, P_{surv}(E_\mu^{'}, E_\mu^{th}, X) \tag{6}$$

where the integral is evaluated from the μ energy losses. We have used the energy loss calculation by Lohmann *et al.* (59) using standard rock for muon energies up to 10^5 GeV. For higher energies we use the approximate formula:

$$\frac{dE_\mu}{dX} = \alpha + \beta \cdot E_\mu\,, \tag{7}$$

where $\alpha \sim 2.0$ MeV g^{-1} cm^2 takes into account the continuous ionization losses and $\beta \sim 3.9 \cdot 10^{-6}$ g^{-1} cm^2 takes into account the stochastic losses due to bremsstrahlung, pair production and nuclear interactions.

The flux of neutrino induced muons detected by an apparatus for a source of declination δ and for a neutrino spectrum $\Phi_\nu(E_\nu) \propto E^{-\gamma}$ is:

$$\Phi_\mu(E_\mu^{th}, E_\nu, \delta) = N_A \int_{E_\mu^{th}}^{E_\mu^{max}} \frac{d\sigma_\nu}{dE_\mu^{'}}(E_\mu^{'}, E_\nu) \cdot R_{eff}(E_\mu^{'}, E_{th}^\mu) \cdot Area(E_\mu^{'}, \delta) \cdot \Phi_\nu(E_\nu)\, dE_\mu^{'}\,. \tag{8}$$

The effective area of the detector $Area(E_\mu^{'}, \delta)$, averaged over 24 hours, depends on the source declination. In the low energy region, the effective area increases with increasing muon energy because not all muons are detected depending on their track length in the detector. At higher energies (in MACRO for $E_\mu \gtrsim 3$ GeV) it reaches a plateau when all muons from all directions have enough energy to be detected. At very high energies the effective area can decrease due to electromagnetic showers. As a matter of fact, the efficiency of the analysis cuts can decrease due

to high track multiplicities for high energy events. Moreover the presence of showers could lead to a bad reconstruction of the neutrino induced muon with another track of the shower. From Monte Carlo studies, the MACRO average effective area begins to decrease for $E_\mu \gtrsim 1$ TeV and it is about 20% (42%) lower at 10 TeV (100 TeV) with respect to 10 GeV. The average area as a function of declination for various energies is shown in Fig. 5. It has been obtained using the detector simulation based on GEANT (60), but modified to properly treat the stochastic muon energy losses above 10 TeV (61). To obtain large Monte Carlo statistics we have used "beams" of monoenergetic muons intercepting isotropically from the lower hemisphere a volume containing MACRO and more than 2 m of the surrounding rock (to evaluate the effect of electromagnetic showers induced by high energy muons). For each beam energy, we have simulated about 10^5 muons.

Due to the increasing value of the ν cross-section, at high energies neutrinos are "absorbed" by the large amount of material they cross through the Earth. Neutrino absorption in the Earth can be taken into account introducing in the integral in eq. 8 the exponential factor:

$$e^{-N_A \cdot \sigma_\nu(E) \cdot X(\cos\theta)} \tag{9}$$

which depends on $X(\cos\theta)$, the quantity of matter transversed by the incident neutrino in the Earth and hence on its zenith angle. The differential number of neutrinos as a function of the neutrino energy (response curves) for a source of differential spectral index $\gamma = 2.1$ at two different declinations with and without absorption in the Earth is shown in Fig. 6. The median neutrino energy is about 15 TeV, while for the atmospheric neutrinos it is between 50-100 GeV (53). It is noticeable how the absorption becomes negligible for sources seen near the horizon ($\delta \sim 0^\circ$). In Fig. 7 the same response curves are shown for 3 spectral indices. In these plots, the normalization of the neutrino fluxes is arbitrary.

It is relevant to notice that if muon neutrinos oscillate into tau neutrinos, as atmospheric neutrino experiment results suggest (53; 62), ν_τ are subject to considerably less absorption than muon neutrinos (63). Tau neutrinos are subject to a regeneration effect in the Earth: ν_τ interacts and the produced tau lepton immediately decays with negligible energy loss; hence from τ decay another ν_τ is produced. This effect, more noticeable for harder spectra, has been neglected here.

The fluxes of detectable upward-going muons for sources with $\gamma = 2.1$ and $\delta = -60^\circ, 0^\circ$ are shown with and without absorption in Fig. 8. If one assumes that the normalization of the neutrino flux is of the order of the upper limits from γ-ray experiments at ~ 100 TeV (2×10^{-13} cm^{-2} s^{-1} for the Galactic Center), the expected rate of neutrino induced muons varies between $10^{-2} \div 10^{-3}$ ($10^{-1} \div 10^{-2}$) events/yr/1000 m^2 for $\gamma = 2.1$ (2.5) depending on the declination of the source. Note that the softer the source spectrum, the higher the neutrino event rates.

An important quantity in the search for celestial point sources is the effective angular spread of the detected muons with respect to the neutrino direction. We have computed the angle between the neutrino and the detected muon using a Monte Carlo simulation. We have assumed a neutrino energy flux of the form $dN/dE_\nu = constant \times E^{-\gamma}$, for several neutrino spectral indices γ, and

considered the neutrino cross-sections, the muon energy loss in the rock and the detector angular resolution. Tab. 2 shows the fraction of the events in a 3° search half-cone for two different spectral indices as a function of the zenith angle. With the simulations of monoenergetic muon beams on a box larger than the detector including ~ 2 m of rock, we have calculated the effective area and even checked that our intrinsic resolution does not worsen with energy due to the effect of increasing electromagnetic showers induced by stochastic energy losses of muons. Up to 100 TeV the average angle between the generated muons and the reconstructed ones is less than 1°.

5. Search for point-like sources

The MACRO data sample is shown in equatorial coordinates (right ascension in hours and declination in degrees) in Fig. 9. For the point-like source search using the direction information of upward-going muons, we evaluate the background due to atmospheric neutrino induced muons randomly mixing for 100 times the local angles of upward-going events with their times. The number of mixings is chosen to have a statistical error for the background about 10 times smaller than the data fluctuations. The local angles are then smeared by $\pm 10°$ in order to avoid repetitions, particularly in the declination regions where there is small acceptance. The value of 10° is chosen to have variations larger than the dimensions of the search cones.

For a known candidate point-like source S the background in the search cone $\Delta\Omega = \pi\omega^2$, with ω the half width of the search cone in radians, is evaluated counting the events in a declination band around the source declination δ_S of $\Delta\delta = \pm 5°$:

$$N_{back} = \frac{N(\Delta\delta)\Delta\Omega}{2\pi[\sin(\delta_S + 5°) - \sin(\delta_S - 5°)]} \,. \tag{10}$$

We have considered the case of a possible detection of an unknown source represented by an excess of events clustered inside cones of half widths 1.5°, 3° and 5°. Hence we have looked at the number of events falling inside these cones around the direction of each of the 1100 measured events. The cumulative result of this search is shown in Fig. 10 for the data (full circles) and the simulation of atmospheric events (solid line). We find 60 clusters of ≥ 4 muons around a given muon (including the event itself), to be compared with 56.3 expected from the background of atmospheric neutrino-induced muons. The largest cluster is made of 7 events in the 3° half-cone and it is located around the equatorial coordinates (right ascension, declination)=$(222.5°, -72.7°)$. Other 2 clusters of 6 events in 3° are located around = $(188.1°, -48.1°)$ and $(342.5°, -74.4°)$, respectively. Nevertheless, they are not statistically significant.

For our search among known point-sources, we have considered several existing catalogues: the recent EGRET catalogue (8), a catalogue of BL Lacertae objects (64) of which 181 fall in the visible sky of MACRO ($-90° \leq \delta \lesssim 50°$), the list of 8 sources in the visible sky emitting photons above TeV already mentioned in Sec. 1, the Green catalogue (65) of SNRs, the BATSE (9) catalogues, 32 *Beppo*SAX GRBs (66), a compilation of 29 Novae X (67), which are binaries with a compact object

and a companion star which transfers mass into an accretion disk. Novae X are characterized by sudden increases of luminosities in the X range ($L \sim 10^{37} - 10^{38}$ erg s^{-1} reached after 20-90 days). Among these catalogues we have selected 42 sources we consider interesting because they have the features required by the "beam dump" model. In Fig. 11 the distribution of the numbers of events falling in the search cones is shown for the data and the simulation for the 42 sources. We find no statistically significant excess from any of the considered sources with respect to the atmospheric neutrino background. For the 42 selected sources we find 11 sources with ≥ 2 events in a search cone of 3° to be compared to 12.0 sources expected from the simulation.

Upper limits on muon fluxes from sources can be calculated at a given confidence level, e.g. 90% c.l. as:

$$\Phi(90\% c.l.) = \frac{\text{Upper limit}(90\% c.l.)}{\text{effective area} \times \text{livetime}}\,, \tag{11}$$

where the numerator is the upper limit calculated from the number of measured events and from the number of expected background events and the denominator is the exposure of the detector which is the area of the apparatus seen by the source during the livetime. Different methods to evaluate upper limits are described in (68). We have calculated the upper limits (the numerator in eq. 11) using the recent and well motivated unified approach by Feldman and Cousins (69). It is possible to calculate neutrino flux upper limits from muon flux upper limits because they are related (see eq. 8). The 90% c.l. muon and neutrino flux limits are given in Tab. 3 for the 42 selected sources. These limits are valid for muon energies > 1 GeV. They include the effect of the absorption of muon neutrino in their propagation through the Earth. The limits are obtained assuming a neutrino spectrum from a source with $\gamma = 2.1$. Moreover, the effect of the decrease in efficiency at very high energies and the reduction factors for a search half-cone of 3° and a spectral index $\gamma = 2.1$ (given in Tab. 2) are included. For comparison we include the best limits from previous experiments. In order to see how the limits depend on the spectral index γ we report in Tab. 4 the percentage difference of the exposure as a function of declination calculated for a source with $\gamma = 2.1$ and a source with $\gamma = 2.3$, 2.5, 2,7, 3.7.

To evaluate the physical implications of our limits we recall that a muon flux of the order of 0.03×10^{-14} cm^{-2} s^{-1} is expected from the supernova remnant Vela Pulsar (34), which predict a yield of neutrinos at the level of about one order of magnitude lower than present limits.

We notice that there are 6 events from GX339-4 in a 3° with chance probability $P = 6 \cdot 10^{-3}$. Considering that we have looked at 42 sources the probability to find such an excess from at least one of these sources is 8.6% (evaluated from Fig. 11).

Between the selected 42 candidate sources, Mkn 421 and Mkn 501 are particularly interesting due to the strong emissions (in the TeV region) they present. These emissions have variable intensity during time. Mkn 421 shows a strongly variable emission with peak flares during June 1995, May 1996 and April 1998 (70). Mkn 501 had a high state emission during about 6 months in 1997, particularly intense between April and September (71). The strongest flare in 1998 occurred on March 5. Unfortunately, the MACRO esposure for this sources is not favoured because they are

seen almost at the horizon where the acceptance is lower. No event from both sources is found inside a search cone as large as 5°. Only two events for each of the sources are found inside 10°. They are of marginal interest due to the large angle with respect to the source directions. They have been measured in periods in which there were not known intense flares (for Mkn 421: 10 Sep. 1996 and 27 Jun. 1998; for Mkn 501: 29 Sep. 1996 and 26 Jun. 1998).

We have also made a search for neutrino signals using a cumulative analysis: for each of several catalogues of source types, we set a limit on flux from sources from that catalogue. In some situations (for example for a uniform distribution in space of sources having the same intensity) this method could give a better sensitivity than the search for a single source. It depends on the spatial distribution and on the intensity of the sources.

We consider the average value N_0 of the distribution for the data and the average value N_B of the distribution for the simulation in Fig. 11 for the 42 sources in the MACRO list, in Fig. 12 for the 220 SNRs, in Fig. 13 for the 181 blazars and in analogous plots for the other catalogues. Then we estimate the cumulative upper limits for N sources in the catalogue as:

$$\Phi_{cumulative}(90\%\text{c.l.}) = \frac{\text{Upper limit}(90\%\text{c.l.})}{\text{Average Area} \cdot \text{livetime}} \tag{12}$$

where the average area is $\frac{\sum_{i=1}^{N} Area(\delta_i)}{N}$, with $Area(\delta_i)$ the area seen by a source with declination δ_i. The upper limit is evaluated for $N_0 > N_B$ as:

$$\text{Upper limit}(90\%\text{c.l.}) = N_0 - N_B + 1.28 \cdot RMS/\sqrt{N} \tag{13}$$

where RMS is the root mean square value of the considered expected distributions and if $N_0 < N_B$ as:

$$\text{Upper limit}(90\%\text{c.l.}) = 1.28 \cdot RMS/\sqrt{N} \tag{14}$$

We obtain $\Phi_{lim}(90\%) = 3.06 \cdot 10^{-16}$ cm^{-2} s^{-1} for the 42 sources in the MACRO list. This can be considered a limit on a diffuse flux.

In the case of the 220 SNRs in the Green catalogue we obtain the cumulative upper limit from the cumulative analysis shown in Fig. 12 of $2.63 \cdot 10^{-16}$ cm^{-2} s^{-1}. This can be considered a diffuse muon flux limit for neutrino production from supernova remnants. For the 181 blazars in (64) (see Fig. 13) we find a cumulative upper limit of the muon flux $5.44 \cdot 10^{-16}$ cm^{-2} s^{-1}. In Tab. 5 we summarize the upper limits for the various catalogues considered.

Finally, it is interesting to note, that most of the models for neutralino annihilation on the Galactic Center in (22) are excluded by our experimental upper limit of $\sim 3 \cdot 10^{-15}$ cm^{-2} s^{-1} when there is a "central spike" for a 3° cone. In Tab. 6 the muon flux limits (90% c.l.) for various search cones around the direction of the Galactic Center (3°, 5° and 10°) for 5 values of the neutralino mass from 60 GeV to 1 TeV are calculated. The dependence of the effective area of the detector as a function of the neutrino energy has been calculated folding with the neutrino flux from neutralino

annihilation calculated by Bottino *et al.* (72). As a first approximation, the difference of using the neutrino fluxes by Silk and Gondolo in the effective area calculation should be negligible. The limits are calculated for $E_\mu > 1$ GeV.

6. Search for correlations with gamma ray bursts

We look for correlations with the gamma ray bursts given in the BATSE Catalogues 3B and 4B (9) containing 2527 gamma ray bursts from 21 Apr. 1991 to 5 Oct. 1999. They overlap in time with 1085 upward-going muons collected by MACRO during this period. The effective area for upward-going muon detection in the direction of the bursts averaged over all the bursts in the catalogue is 121 m^2. Its value is small because our detector is sensitive to neutrinos only in one hemisphere and because it was not complete in the period 1991-1994. Fig. 14 shows our neutrino events and BATSE GRBs as a function of the year.

We find no statistically significant correlation between neutrino events and gamma burst directions for search cones of 10°, 5° and 3° half widths. The width of the search cones is related to the BATSE angular resolution; these cones include 96.9%, 85.1% and 70.5% neutrinos respectively if emitted from GRBs. These numbers do not include the contributions due to the muon-neutrino angle, to the muon propagation in the rock or to the MACRO angular resolution, which are small with respect to BATSE angular resolution.

We also consider possible time correlations between MACRO and BATSE events. For the temporal coincidences we use both the position information and the time information. In order to calculate the background we add 200 temporal shifts to the time difference between the event detected by other experiments and the ν event in MACRO considering various time intervals (the minimum interval is [-4000 s, 4000 s], the maximum interval is [-80000 s, 80000 s]). We consider time windows of $\pm$400 s every 20 s.

We find one event after 39.4 s from the 4B950922 γ-ray burst of 22 Sep. 1995 at an angular distance of 17.6° and another very horizontal event in coincidence with the 4B940527 γ-ray burst of 27 May 1994 inside 280 s at 14.9°. The 90% c.l. muon flux limit is calculated for a search cone of 10° around the gamma burst direction and in an arbitrary time window of $\pm$200 s. The choice of this time window is arbitrary because one does not know *a priori* what the duration of the neutrino emission is. Models of GRB emitters are not yet clear in predicting when and for how long neutrinos are emitted. This is in fact the reason why we have considered even a directional analysis of GRBs using no time information (see previous section). On the other hand, in this section we are using the time information and our choice of the time window where we set the upper limit is only motivated by the fact that this window is larger than the duration of 97.5% of the 3B Catalogue GRBs (for which the measured durations are available). In the chosen search window we find no events to be compared to 0.04 expected background events. Fig. 15 shows the difference in time between the detection of an upward-going muon and a GRB as a function of the

cosine of their angular separation. Two scales are shown: the upper plot is an expanded scale of the lower one.

The corresponding flux upper limit (90% c.l.) is 0.79×10^{-9} cm^{-2} upward-going muons per average burst. The limit is almost eight orders of magnitude lower than the flux coming from an "extreme" topological defect model reported in (43), while according to a model in the context of the fireball scenario (44) a burst at a distance of 100 Mpc producing 0.4×10^{51} erg in neutrinos of about 10^{14} eV would produce $\sim 6 \times 10^{-11}$ cm^{-2} upward going muons.

The same analysis on space and time correlations has been performed for 32 *Beppo*SAX events; the result is compatible with the atmospheric neutrino background.

7. Conclusions

We have investigated the possibility that the sample of 1100 upward-going muons detected by MACRO since 1989 shows evidence of a possible neutrino astrophysics source. We do not find any significant signal with respect to the statistical fluctuations of the background due to atmospheric neutrinos from any of the event directions or from any candidate sources. We also used the time information to look for correlations with gamma-ray bursts detected by BATSE and *Beppo*SAX. Having found no excess of events with respect to the expected background we set muon and neutrino flux upper limits for point-like sources and for the cumulative search for catalogues of sources. These limits have been calculated taking into account the response of MACRO to various neutrino fluxes from candidate sources until energies $\gtrsim 100$ TeV. These limits are for almost all of the considered sources the most stringent ones compared to other current experiments. They are about 1 order of magnitude higher than values quoted by most plausible neutrino source models except for the model in (22) which is seriously constrained.

Acknowledgements

We gratefully acknowledge the support of the director and of the staff of the Laboratori Nazionali del Gran Sasso and the invaluable assistance of the technical staff of the Institutions participating in the experiment. We thank the Istituto Nazionale di Fisica Nucleare (INFN), the U.S. Department of Energy and the U.S. National Science Foundation for their generous support of the MACRO experiment. We thank INFN, ICTP (Trieste) and NATO for providing fellowships and grants for non Italian citizens.

REFERENCES

K. Greisen, Phys. Rev. Lett. **16** (1966) 748; G. T. Zatsepin and V. A. Kuz'min, Pisma Zh. Eksp. Teor. Fiz. **4** (1966) 114.

K. Greisen, Ann. Rev. Nucl. Science **10** (1960) 1.

J. N. Bahcall and S. C. Frautschi, Phys. Rev. **135** (1964) 788.

R. Davis Jr., D. S. Harmer and K. C. Hoffman, Phys. Rev. Lett. **20** (1968) 1205.

K. Hirata *et al.*, Phys. Rev. Lett. **58** (1987) 1490.

R. M. Bionta *et al.*, Phys. Rev. Lett. **58** (1987) 1494.

J. D. Jackson, H. E. Gove and V. Lüth, Ann. Rev. Nucl. Part. Sci. **43** (1993) 883.

R. C. Hartman *et al.*, can be downloaded from the
URL : ftp : //gamma.gsfc.nasa.gov/pub/THIRD_CATALOG/.

W.S. Paciesas *et al.*, *The fourth BATSE Gamma-Ray burst Catalog*, astro-ph/9903205 (1999); the current BATSE Catalog can be downloaded at the URL:http://gammaray.msfc.nasa.gov/batse/.

F. Frontera, *Recent results on gamma ray bursts with the BEPPOSAX satellite*, highlight paper, in Proc. of 25^{th} Int. Cosmic Ray Conf. (ICRC 97), Durban, South Africa, 28 Jul. - 8 Aug. 1997, Vol. **8**, 307.

J. E. McEnery *et al.*, *First results of a study of TeV emission from GRBs in Milagrito*, astro-ph/9910549 (1999).

M. J. Lang *et al.*, Nucl. Phys. Proc. Suppl. **14A** (1990) 165.

T. Yoshikoshi *et al.*, Astrophys. J. **487** (1997) L65.

T. Tanimori *et al.*, *Discovery of TeV gamma rays from SN1006: further evidence for the SNR origin of cosmic rays*, astro-ph/9801275, submitted to Astrophys. J. Lett. (1998).

M. Punch *et al.*, Nature **358** (1992) 477.

D. Petry *et al.*, *AGN studies above 1.5 TeV with the Hegra 5 m^2 Cherenkov telescope*, Proc. of the 25^{th} Int. Cosmic Rays Conf., 28 Jul. - 8 Aug. 1997, Durban, South Africa, Vol. **3**, 241.

J. Quinn *et al.*, Astrophys. J. **456** (1996) L83.

P. M. Chadwick *et al.*, Astrophys. J. **513** (1999) 161.

T. Kifune *et al.*, Astrophys. J. **438** (1995) L91.

Sako *et al.*, *Observations of pulsars, PSR1509-58 and PSR1259-63 by CANGAROO 3.8 m telescope*, Proc. of the 25^{th} Int. Cosmic Rays Conf., 28 Jul. - 8 Aug. 1997, Durban, South Africa, Vol. **3**, 193.

A. M. Hillas, Rapporteur Talk at the 24^{th} Cosmic Ray Conference, 28 Aug.-8 Sep. 1995, Roma, 701 (1995).

P. Gondolo and J. Silk, Phys. Rev. Lett. **83** (1999) 1719.

H. Adarkar *et al.*, KGF Collaboration, Astrophys. J. **380** (1991) 235; *Point source search at great underground depth*, Proc. of the 24^{th} Int. Cosmic Rays Conf., 28 Aug. - 8 Sep. 1995, Roma, Vol. **1**, 820.

R. Svoboda *et al.*, IMB Collaboration, Astrophys. J. **315** (1987) 420; R. Becker-Szendy *et al.*, Astrophys. J. **444** (1995) 415, R. Becker-Szendy *et al.*, Nucl. Phys. **B** (Proc. Suppl.) **38** (1995) 331.

Y. Oyama *et al.*, Phys. Rev. **D39** (1989) 1481.

M. M. Boliev *et al.*, Baksan Collaboration, *Search for astrophysical sources of neutrinos and neutrino oscillations using the Baksan data*, Proc. of the 24^{th} Int. Cosmic Rays Conf., 28 Aug. - 8 Sep. 1995, Roma, Vol. **1**, 722.

K. John for the AMANDA Collaboration, *A search for point sources of high energy neutrinos with the AMANDA neutrino telescope*, Proc. of the 26^{th} Int. Cosmic Rays Conf., 17-25 Aug. 1999, Salt Lake City, Utah, Vol. **2**, 196.

V. S. Berezinsky, C. Castagnoli and P. Galeotti, Il Nuovo Cimento **8C** (1985) 185.

T. K. Gaisser, F. Halzen and T. Stanev, Phys. Rep. **258** (1995) 173.

M. S. Longair, *High Energy Astrophysics. Vol. 1: Particles, Photons and their detection*, ed. Cambridge Univ. Pr. (1994).

W. Rhode *et al.*, Frejus Collaboration, Astropart. Phys. **4** (1996) 217.

V. A. Balkanov *et al.*, *Search for high-energy neutrinos with the Baikal underwater detector NT-96*, to appear in Proc. of 2^{nd} Int. Conf. Physics Beyond the Standard Model: Beyond the Desert 99: Accelerator, NonAccelerator and Space Approaches, Ringberg Castle, Tegernsee, Germany, 6-12 Jun 1999 and astro-ph/9910133.

A. Corona, for the MACRO Collaboration, Proceedings of the 24^{th} Int. Cosmic Rays Conf., 28 Aug.-8 Sep. 1995, Roma, Vol. 1, 800.

T. K. Gaisser, Nucl. Phys. **B** (Proc. Suppl.) **48** (1996) 405.

R. J. Protheroe, W. Bednarek and Q. Luo Astrop. Phys. **9** (1998) 1.

G. Sigl, S. Lee,D. N. Schramm and P. Coppi, Phys. Lett. **B392** (1997) 129.

F. Halzen, *Lectures on neutrino astronomy: theory and experiment*, lectures given at Theoretical Advanced Study Institute in Elementary Particle Physics (TASI 98): "Neutrinos in Physics and Astrophysics: from 10^{-33} to 10^{28} cm", Boulder, CO, 31 May- 26 Jun. 1998 and astro-ph/9810368.

F. W. Stecker, C. Done, M. H. Salamon and P. Sommers, Phys. Rev. Lett. **66** (1991) 2697, Erratum-ibid. **69** (1992) 2738

A. P. Szabo and R. J. Protheroe, Astropart. Phys. **2** (1994) 375

E. Costa *et al.*, IAU Circular n. 6576 (1997).

M. R. Metzger *et al.*, Nature **387** (1997) 878.

T. Piran, Phys. Rep. **314** (1999) 575.

F. Halzen and G. Jaczo, Phys. Rev. **D54** (1996) 2779.

E. Waxman and J. N. Bahcall, Phys. Rev. Lett. **78** (1997) 2292.

J. P. Rachen and P. Meszaros, Phys. Rev. **D58** (1998) 123005.

M. Vietri, Phys. Rev. Lett. **80** (1998) 3690.

E. Waxman and J. N. Bahcall, Phys. Rev. **D59** (1999) 023002.

F. Halzen and D. W. Hooper, *Neutrino Event Rates from gamma ray bursts*, astro-ph/9908138 (1999).

K. Mannheim, R. J. Protheroe and J.P. Rachen, *On the cosmic ray bound for models of extragalactic neutrino production*, astro-ph/9812398, submitted to Phys. Rev. **D**.

S. P. Ahlen *et al.*, MACRO Collaboration, Nucl. Instr. Meth.**A324** (1993) 337.

M. Ambrosio *et al.*, MACRO Collaboration, Phys. Rev. **D59** (1999) 012003.

M. Ambrosio *et al.*, MACRO Collaboration, Phys. Lett. **B357** (1995) 481.

M. Ambrosio *et al.*, MACRO Collaboration, Phys. Lett. **B434** (1998) 451.

M. Ambrosio *et al*, MACRO Collaboration, Astropart. Phys. **9** (1998) 105.

G. Wolf, Nucl. Phys. **B** (Proc. Suppl.) **38** (1995) 107.

R. Gandhi, C. Quigg, M. Hall Reno and I. Sarcevic, Astropart. Phys. **5** (1996) 81; Phys. Rev. **D58** (1998) 093009.

H. Lai *et al.*, CTEQ Collaboration, Phys. Rev. **D51** (1995) 4763.

H. Plothow-Besch, Comput. Phys. Commun. **75** (1993) 396.

W. Lohmann, R. Kopp and R. Voss, CERN Yellow Report CERN 85-03 (1985).

R. Brun *et al.*, CERN report DD/EE/84-1 (1987).

S. Bottai and L. Perrone, *Simulation of UHE muons propagation for GEANT3*, hep-ex/0001018 (2000).

Y. Fukuda *et al.*, Super-Kamiokande Collaboration, Phys. Rev. Lett. **82** (1999) 2644.

F. Halzen and D. Saltzberg, Phys. Rev. Lett. **81** (1998) 4305 and S. Bottai and F. Becattini, Proc. of 26^{th} Int. Cosmic Ray Conf., 17-25 Aug. 1999, Salt Lake City, Utah, vol.**2**, p. 249.

P. Padovani and P. Giommi, Mon. Not. R. Astron. Soc. **277** (1995) 1477, available at the URL:http://icarus.stsci.edu/ padovani/

D. A. Green, *A Catalog of Galactic Supernova Remnants*, available at the URL:http://www.mrao.cam.ac.uk/surveys/snrs/

E. Pian, private communication, available at the URL:http://tonno.tesre.bo.cnr.it/ pian.

N. Masetti, private communication.

C. Caso *et al.*, *Review of Particle Physics*, Eur. J. Phys. **C3** (1998) 1.

G. J. Feldman and R. D. Cousins, Phys. Rev. **D57** (1998) 3873.

F. Krennrich *et al.*, *TeV flare spectra of Mkn 421 and Mkn 501* Proc. of the 26^{th} Int. Cosmic Rays Conf., 17-25 Aug. 1999, Salt Lake City, Utah, Vol. **3**, 301.

R. J. Protheroe *et al.*, *Very high energy gamma rays from Markarian 501*, 25^{th} Int. Cosmic Rays Conf., 28 Jul. - 8 Aug. 1997, Durban, South Africa, Highlight Session, vol. 8, p. 317.

A. Bottino, N. Fornengo, G. Mignola, and L. Moscoso, Astropart. Phys. **3** (1995) 65.

Table 1: Values of the probability (given in eq. 5) for a neutrino or antineutrino producing a muon with energy larger than the energy threshold of 1 GeV as a function of the neutrino energy.

E_ν (GeV)	$P_{\nu\to\mu^-}$	$P_{\bar{\nu}\to\mu^+}$
10	8.15×10^{-11}	4.88×10^{-11}
10^2	9.05×10^{-9}	5.87×10^{-9}
10^3	5.79×10^{-7}	3.86×10^{-7}
10^4	1.52×10^{-5}	1.09×10^{-5}
10^5	1.35×10^{-4}	1.17×10^{-4}

Table 2: Fraction of events inside a cone of 3° half width for 2 spectral indices and for 5 zenith angles.

$\cos\theta$	$\gamma=2$	$\gamma=2.2$
0.15	0.77	0.72
0.35	0.90	0.85
0.55	0.91	0.87
0.75	0.91	0.87
0.95	0.91	0.87

Table 3. 90% c.l. neutrino induced μ-flux limits for the MACRO list of 42 sources. Corresponding limits on the neutrino flux are given in the last column. These limits are calculated for $\gamma = 2.1$ and for $E_\mu > 1$ GeV including the decrease in efficiency at very high energies. The reduction factors for a 3° half width cone are included. These limits include the effect of absorption of neutrinos in the Earth. The flux upper limits are calculated with the unified approach of Feldman & Cousins (69). B indicates the results of Baksan (26); I the results of IMB (24).

Source	δ (degrees)	Events in 3^o	Backg. in 3^o	ν induced μ-Flux Limits (10^{-14} cm^{-2} s^{-1})	Previous best μ limits (10^{-14} cm^{-2} s^{-1})	ν-Flux limits (10^{-6} cm^{-2} s^{-1})
SMC X-1	-73.5	3	2.1	0.62	-	1.18
LMCX-2	-72.0	0	2.0	0.15	-	0.33
LMCX-4	-69.5	0	2.0	0.15	0.36 B	0.29
SN1987A	-69.3	0	2.0	0.15	1.15 B	0.31
GX301-2	-62.7	2	1.8	0.53	-	1.10
Cen X-5	-62.2	2	1.7	0.55	-	1.04
GX304-1	-61.6	2	1.7	0.54	-	1.05
CENXR-3	-60.6	1	1.7	0.36	0.98 I	0.68
CirXR-1	-57.1	5	1.7	1.18	-	2.21
2U1637-53	-53.4	0	1.7	0.19	-	0.36
MX1608-53	-52.4	0	1.7	0.20	-	0.38
GX339-4	-48.8	6	1.7	1.62	-	3.00
ARA XR1	-45.6	3	1.6	1.00	-	1.87
VelaP	-45.2	1	1.5	0.51	0.78 I	0.94
GX346-7	-44.5	0	1.5	0.23	-	0.43
SN1006	-41.7	1	1.3	0.56	-	1.04
VelaXR-1	-40.5	0	1.3	0.26	0.45 B	0.55
2U1700-37	-37.8	1	1.3	0.58	-	1.08
L10	-37.0	2	1.1	0.91	-	1.72
SGR XR-4	-30.4	0	0.9	0.34	-	0.63
Gal Cen	-28.9	0	0.9	0.34	0.95 B	0.65
GX1+4	-24.7	0	0.9	0.36	-	0.67
Kep1604	-21.5	2	0.9	1.12	-	2.12
GX9+9	-17.0	0	0.9	0.40	-	0.75
Sco XR-1	-15.6	1	0.9	0.85	1.5 B	1.59
Aquarius	-1.0	4	0.8	2.48	-	4.66
4U0336+01	0.6	1	0.8	1.17	-	2.19
AQL XR-1	0.6	0	0.8	0.57	-	1.18
2U1907+2	1.3	0	0.8	0.58	-	1.27
SER XR-1	5.0	0	0.7	0.67	-	1.41

Table 3—Continued

Source	δ (degrees)	Events in 3^o	Backg. in 3^o	ν induced μ-Flux Limits (10^{-14} cm^{-2} s^{-1})	Previous best μ limits (10^{-14} cm^{-2} s^{-1})	ν-Flux limits (10^{-6} cm^{-2} s^{-1})
SS433	5.7	0	0.7	0.67	1.8 B	1.27
2U0613+09	9.1	1	0.6	1.52	-	3.02
Geminga	18.3	0	0.5	1.12	3.1 I	2.10
Crab	22.0	1	0.4	2.52	2.6 B	4.70
2U0352+30	31.0	2	0.3	5.98	-	11.43
Cyg XR-1	35.2	0	0.2	3.24	-	6.24
Her X-1	35.4	0	0.2	3.30	4.3 I	6.96
Cyg XR-2	38.3	0	0.1	4.99	-	10.61
MRK 421	38.4	0	0.1	5.00	3.3 I	9.56
MKN 501	40.3	0	0.1	5.73	-	10.69
Cyg X-3	40.9	0	0.1	6.59	4.1 I	12.49
Per XR-1	41.5	0	0.1	7.51	-	13.99

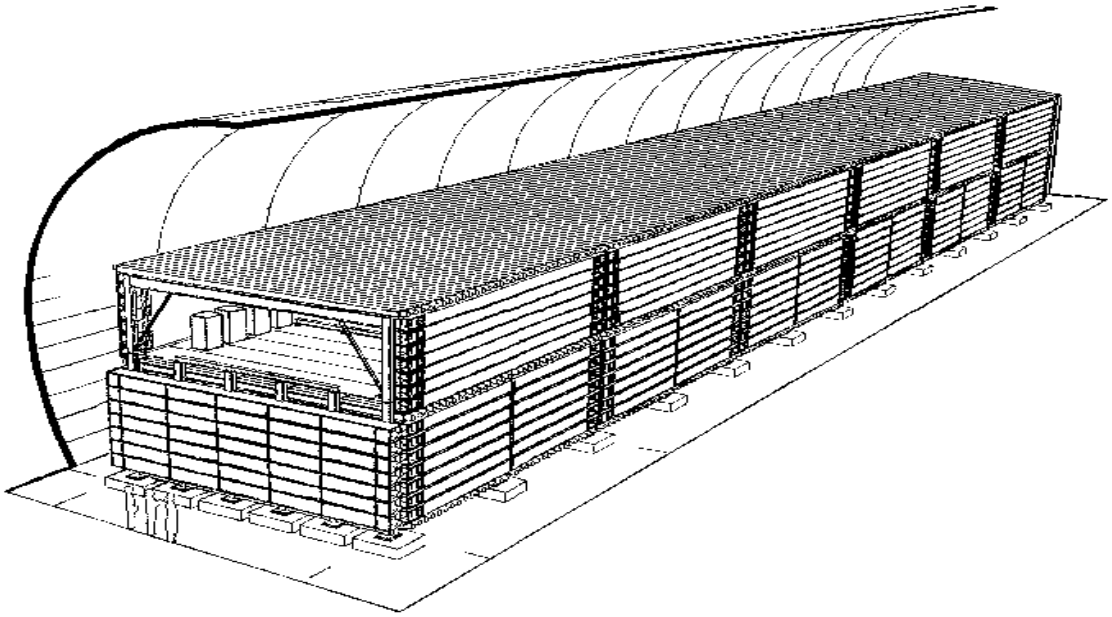

Fig. 1.— Layout of the MACRO detector.

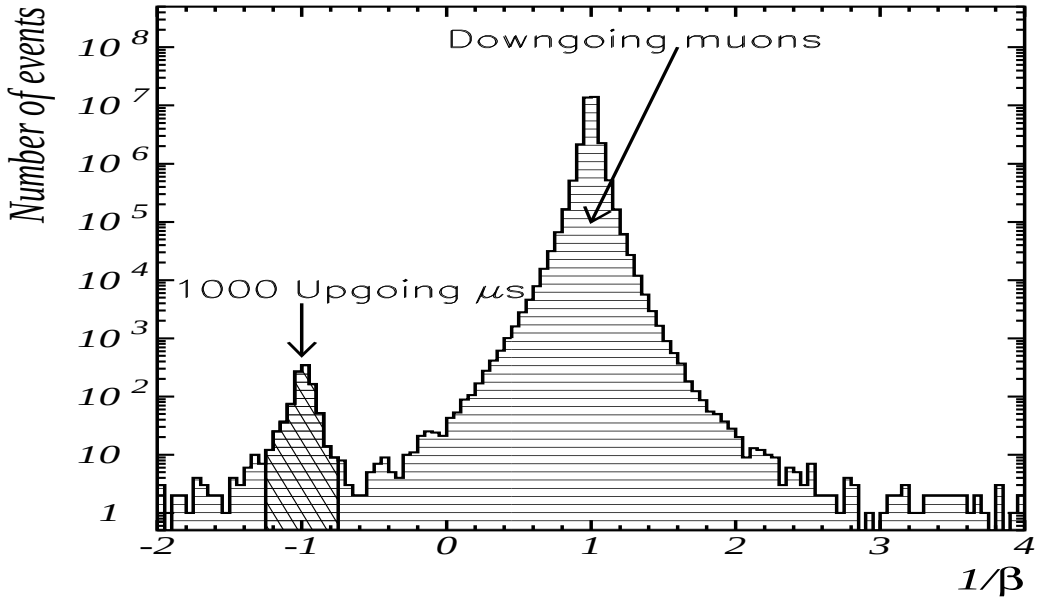

Fig. 2.— The $1/\beta$ distribution for the muon data sample collected with the full detector; the number of downgoing muons is $\sim 33.8 \times 10^6$.

Table 4: Percentage increase (+) or decrease (-) of MACRO exposure between a source producing a neutrino spectrum with $\gamma = 2.3$, 2.5, 2.7 (such in the case of atmospheric neutrinos with $E_\nu \lesssim 10$ GeV) and 3.7 (such in the case of high energy atmospheric neutrinos) with respect to the $\gamma = 2.1$ spectrum.

Declination	Difference (%) $\gamma = 2.3$	Difference (%) $\gamma = 2.5$	Difference (%) $\gamma = 2.7$	Difference (%) $\gamma = 3.7$
$-90°$	+4.1	+5.9	+5.2	−23.8
$-80°$	+2.8	+4.2	+3.9	−18.7
$-70°$	+3.0	+4.6	+4.5	−18.7
$-60°$	+2.9	+4.5	+4.4	−18.9
$-50°$	+2.7	+4.0	+3.6	−19.9
$-40°$	+3.0	+4.6	+4.4	−18.6
$-30°$	+3.0	+4.5	+4.2	−19.0
$-20°$	+3.0	+4.4	+3.9	−20.0
$-10°$	+3.3	+4.9	+4.4	−20.4
$0°$	+3.7	+5.6	+5.3	−19.5
$10°$	+3.8	+5.8	+5.7	−19.5
$20°$	+4.1	+6.6	+7.1	−15.8
$30°$	+5.1	+7.8	+7.8	−17.2
$40°$	+5.0	+7.4	+6.9	−16.7

Table 5: Flux upper limits on muon fluxes from neutrino production for various catalogues at 90% c.l. for $E_\mu > 1$ GeV and for an assumed spectral index of the neutrino flux of $\gamma = 2.1$. The catalogue, the number of souces in it, the average exposure which is the denominator in eq. 12, the muon flux upper limit and the neutrino flux upper limit are given. Flux upper limits are calculated according to eq. 13 and eq. 14.

Catalog	Num. sources	Average Exposure (cm^2 s)	ν-induced μ flux limit ($cm^{-2}s^{-1}$)	ν flux limit ($cm^{-2}s^{-1}$)
MACRO list	42	$4.67 \cdot 10^{14}$	$3.06 \cdot 10^{-16}$	$5.79 \cdot 10^{-8}$
SNRs (65)	220	$2.35 \cdot 10^{14}$	$2.63 \cdot 10^{-16}$	$5.00 \cdot 10^{-8}$
Blazar (64)	181	$2.77 \cdot 10^{14}$	$5.44 \cdot 10^{-16}$	$1.03 \cdot 10^{-7}$
BATSE (9)	2527	$3.37 \cdot 10^{14}$	$1.68 \cdot 10^{-16}$	$3.17 \cdot 10^{-8}$
EGRET (8)	271	$3.66 \cdot 10^{14}$	$2.03 \cdot 10^{-16}$	$3.82 \cdot 10^{-8}$
*Beppo*SAX (66)	32	$3.41 \cdot 10^{14}$	$6.84 \cdot 10^{-16}$	$1.27 \cdot 10^{-7}$
NovaeX (67)	29	$4.97 \cdot 10^{14}$	$5.34 \cdot 10^{-16}$	$1.01 \cdot 10^{-7}$

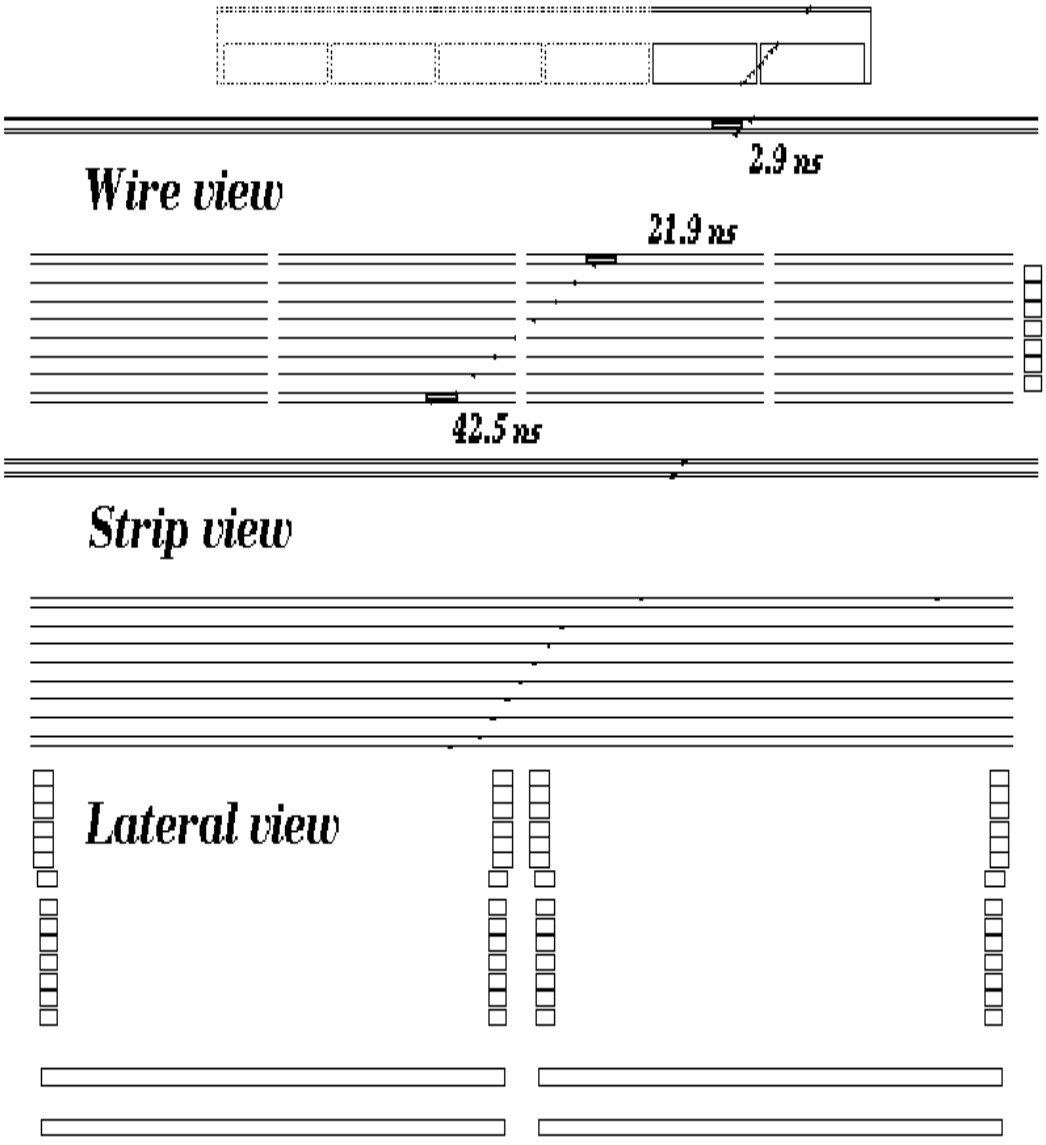

Fig. 3.— One upward-going muon produced by a neutrino interaction in the rock below the MACRO detector. The wire, strip and lateral views are shown and the times in nanoseconds are indicated near the scintillator counters hit by the track. The first hit counter corresponds to the larger time.

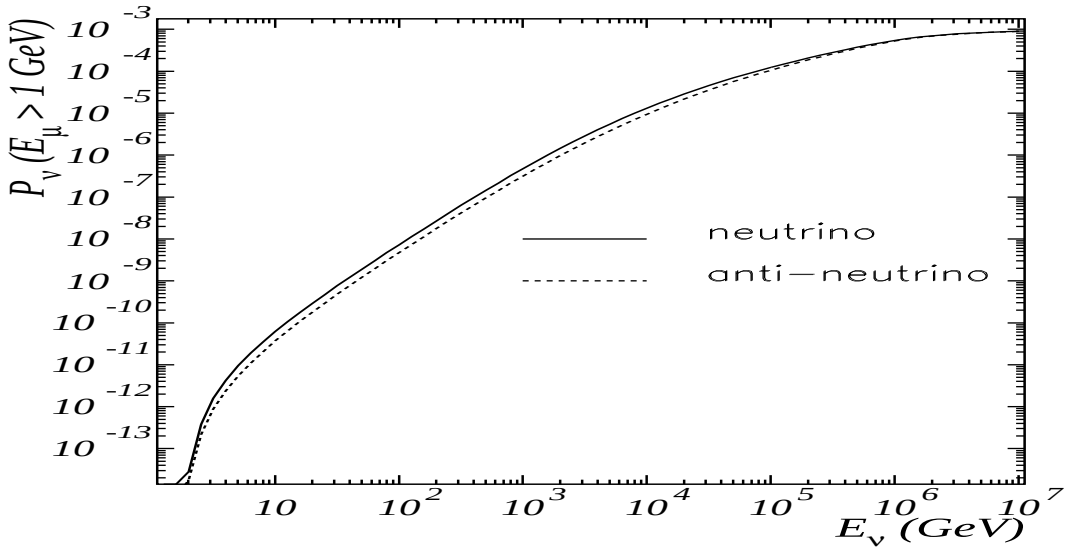

Fig. 4.— Probability that a ν with E_ν crossing the detector produces a muon above threshold. Solid line: neutrino; dotted line: anti-neutrino.

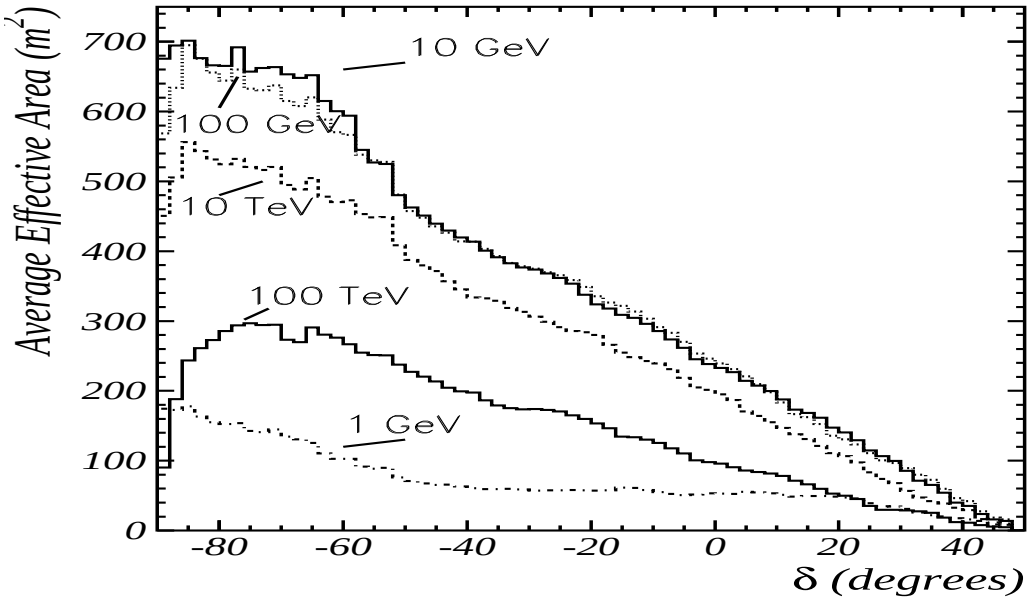

Fig. 5.— MACRO average effective area as a function of declination for various muon energies. From top to bottom lines: 10 GeV (solid line), 100 GeV (dotted line), 10 TeV (dashed line), 100 TeV (solid line) and 1 GeV (dot-dashed line).

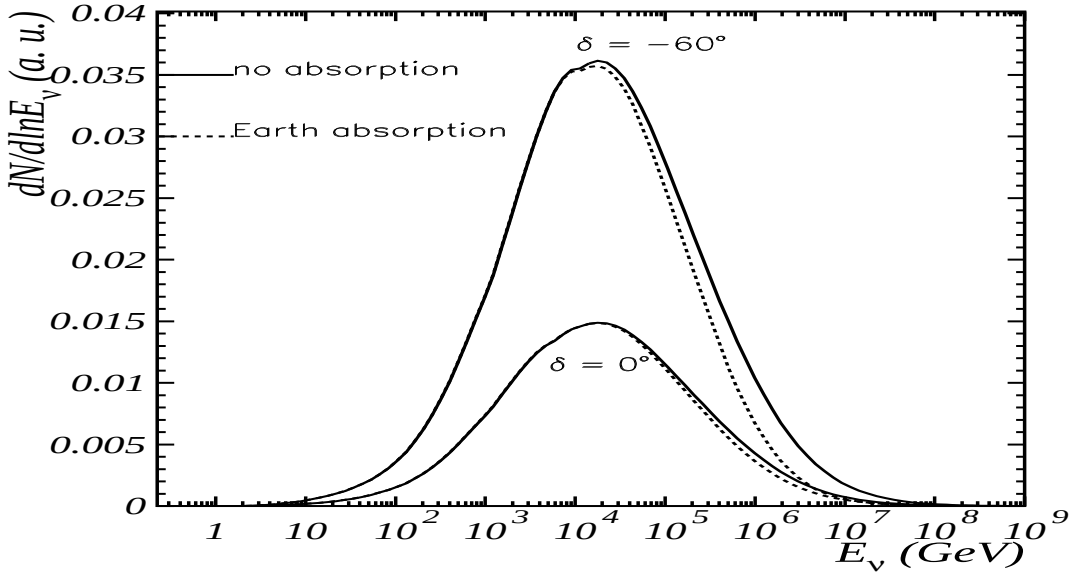

Fig. 6.— MACRO response curve, which is the differential rate of neutrinos which induce detectable muons as a function of the neutrino energy, for 2 sources at declinations $-60°$ and $0°$. Solid (dotted) lines do not (do) include Earth absorption. The normalization of the neutrino fluxes is arbitrary.

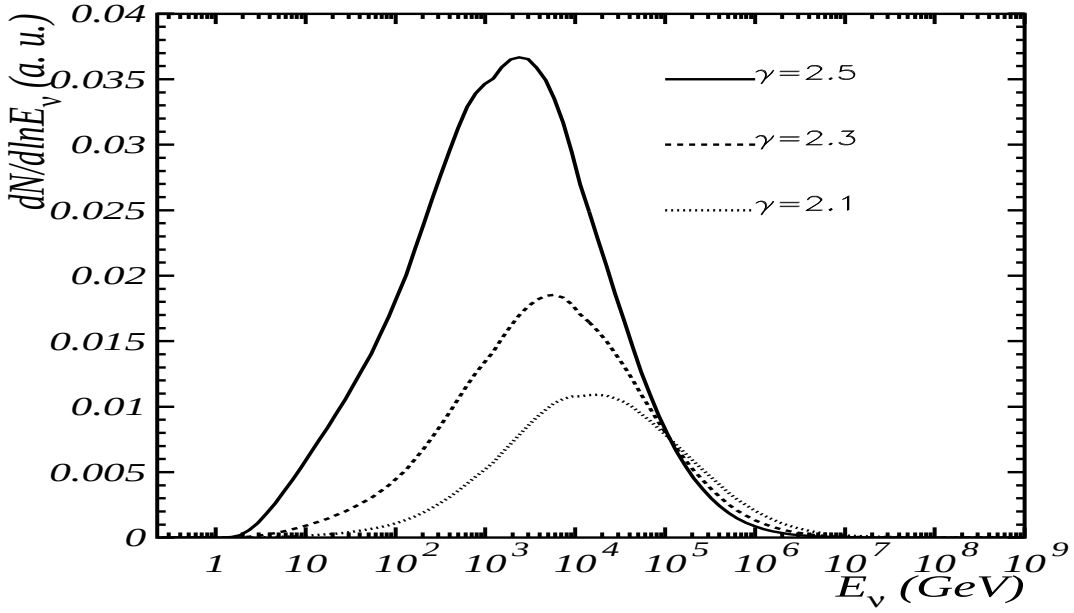

Fig. 7.— MACRO response curves for spectral indices (γ=2.1, 2.3, 2.5) for a source at declination $-60°$. Earth absorption is included.

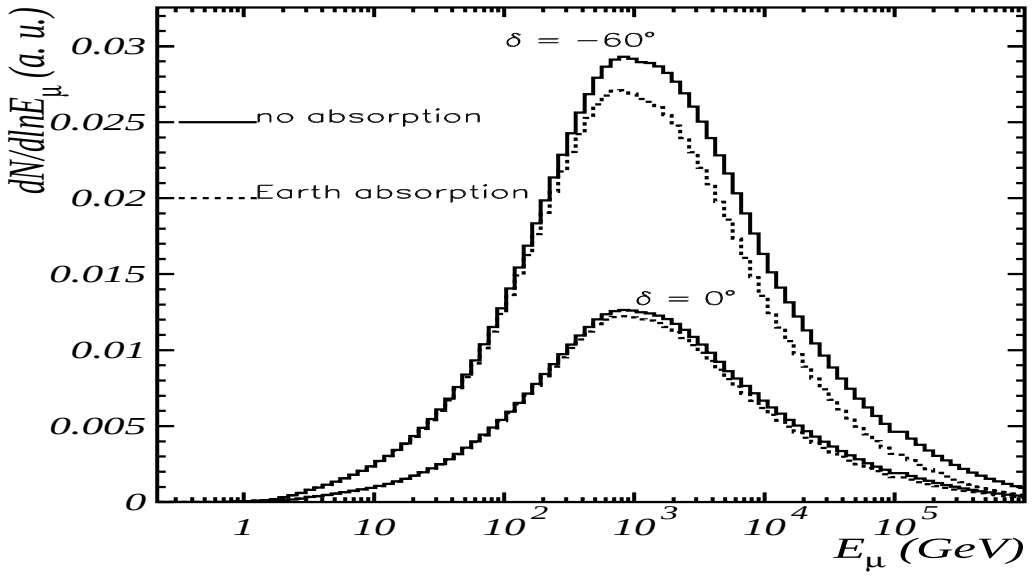

Fig. 8.— Differential rate of detected muons as a function of muon energy in MACRO for spectral indices γ=2.1 and for sources at declinations $-60°$ and $0°$ with (dotted line) and without (solid line) absorption.

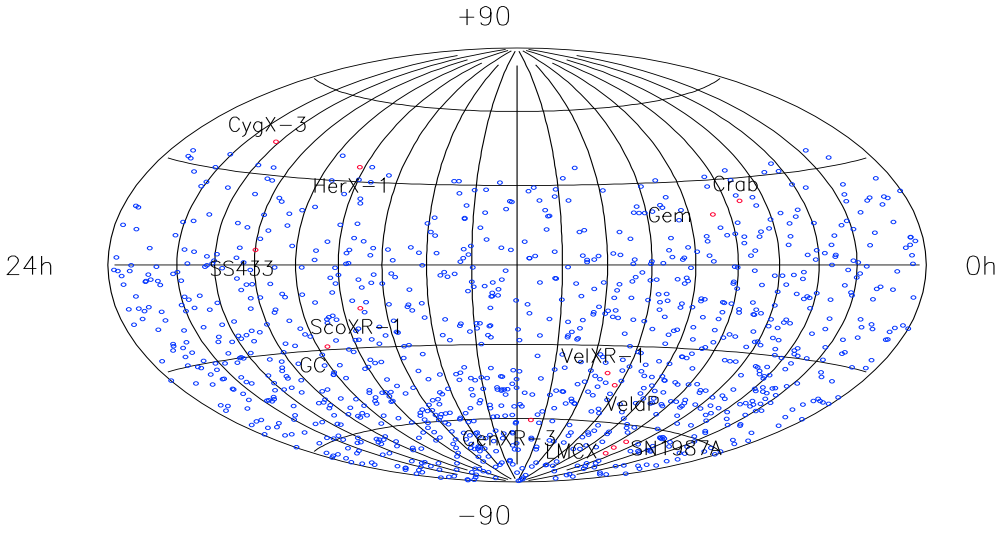

Fig. 9.— Upward-going muon distribution in equatorial coordinates (1100 events).

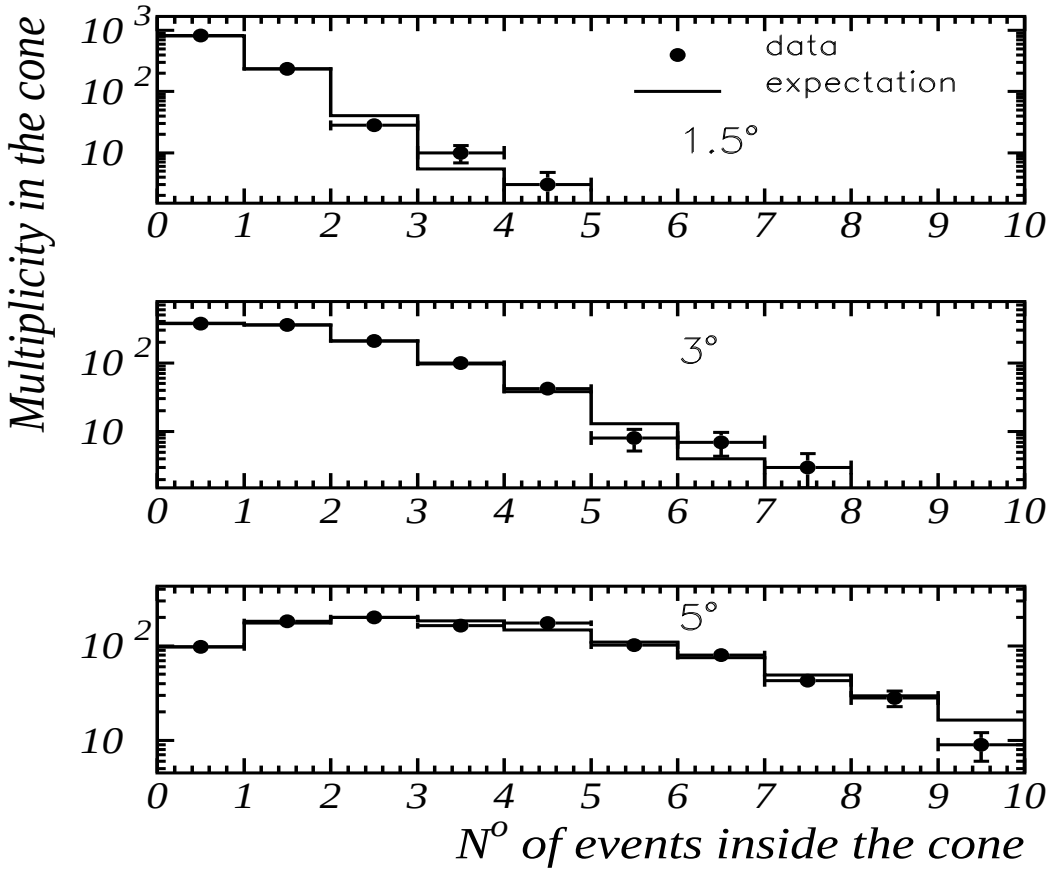

Fig. 10.— On the x axis there is the number of events falling in cones of half width 1.5°, 3°, 5° (from top to bottom plot) around the direction of any muon. The y axis depends on the total number of events considered. Black circles: data. Solid line: simulation.

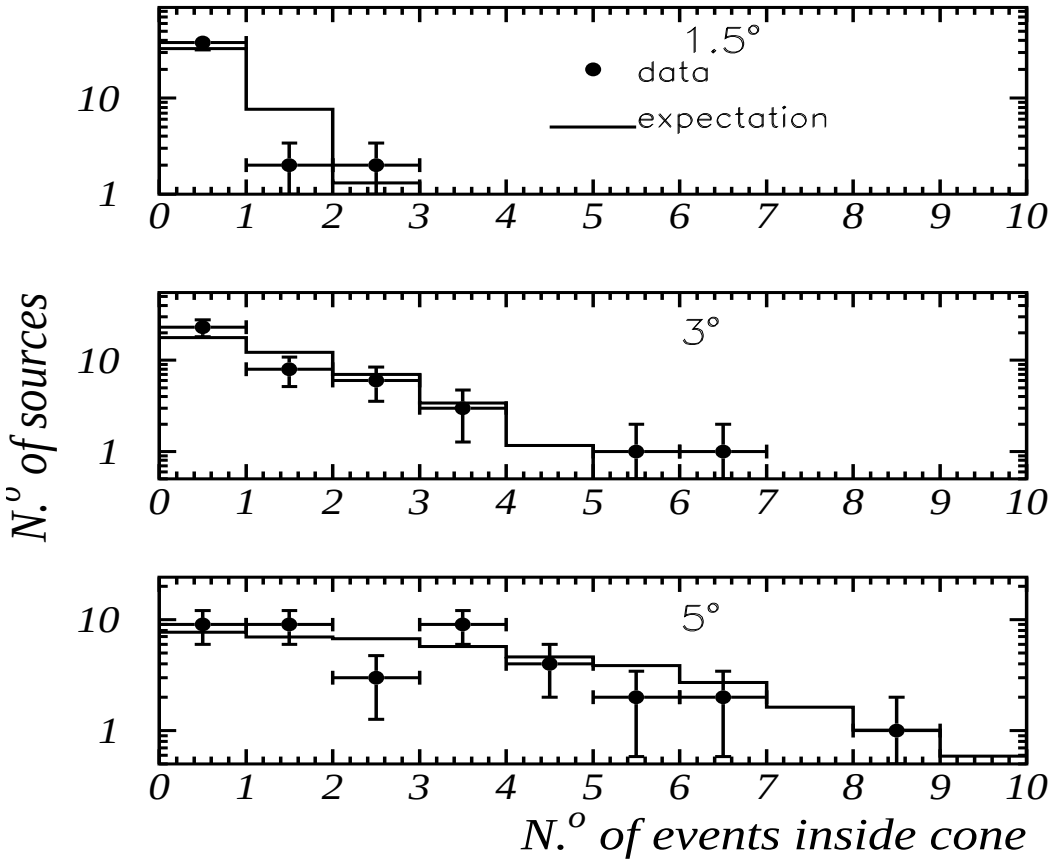

Fig. 11.— On the x axis there is the number of events falling in cones of half width 1.5°, 3°, 5° (from top to bottom) around the direction of the 42 sources considered. The y axis depends on the total number of sources considered. Black circles: data. Solid line: simulation.

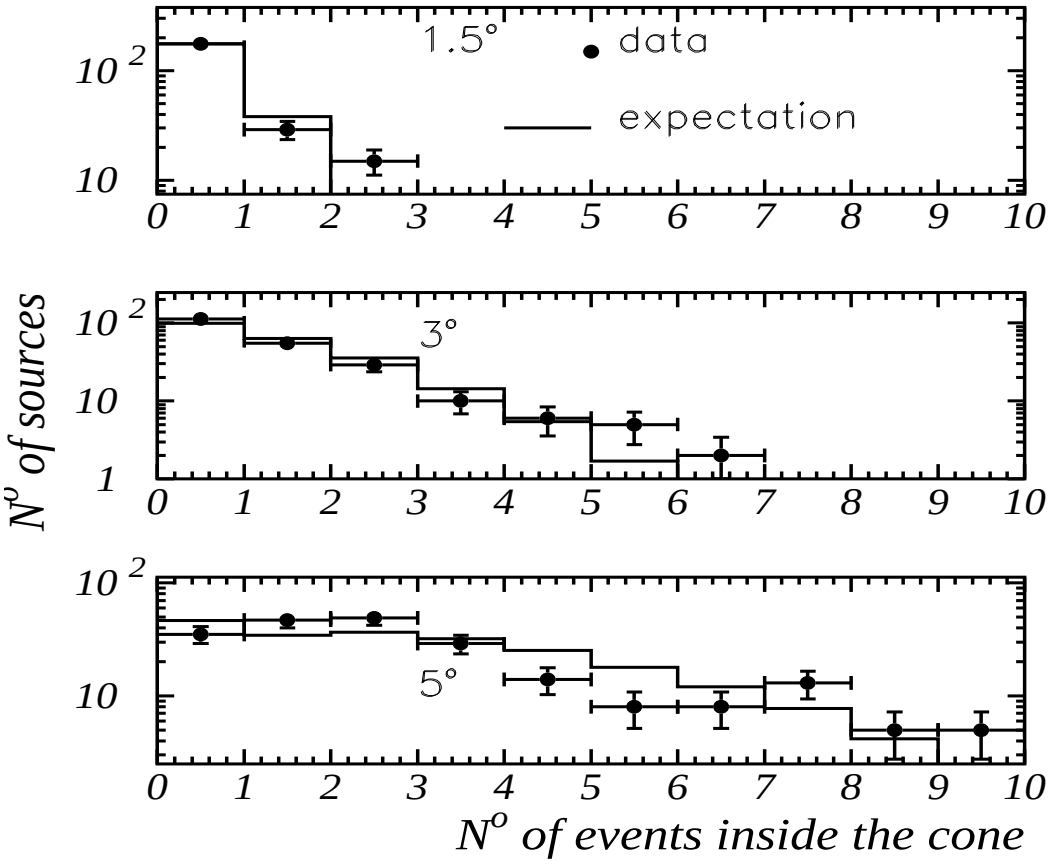

Fig. 12.— On the x axis there is the number of events falling in cones of half width 1.5°, 3°, 5° (from top to bottom) around the direction of 220 SNRs from (65). The y axis depends on the total number of sources considered. Black circles: data. Solid line: simulation.

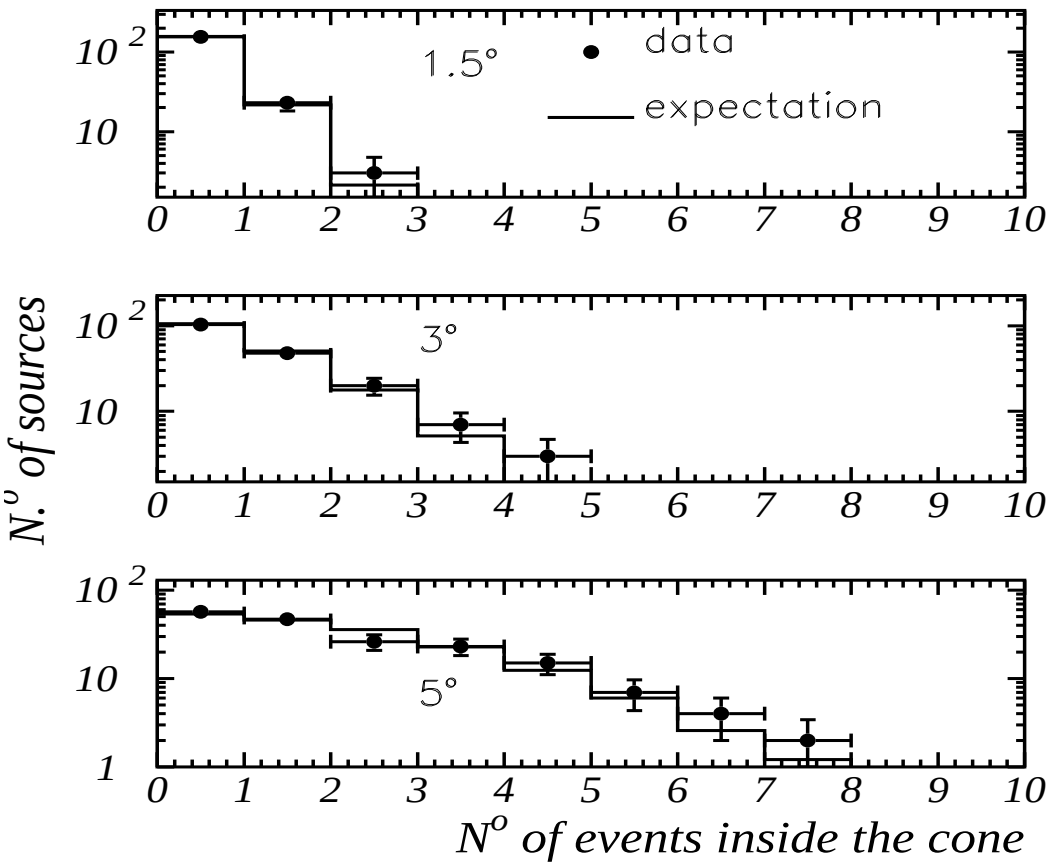

Fig. 13.— On the x axis there is the number of events falling in cones of 1.5°, 3°, 5° around the direction of 181 blazars from (64). The y axis depends on the total number of sources considered. Black circles: data. Solid line: simulation.

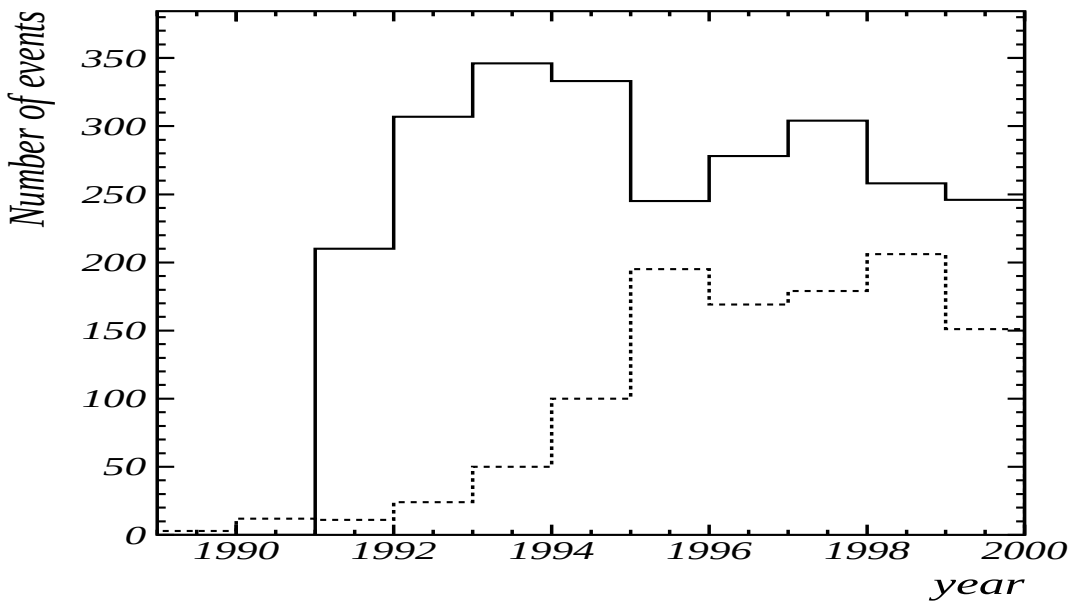

Fig. 14.— MACRO events (dashed line) and BATSE GRBs (solid line) as a function of the year.

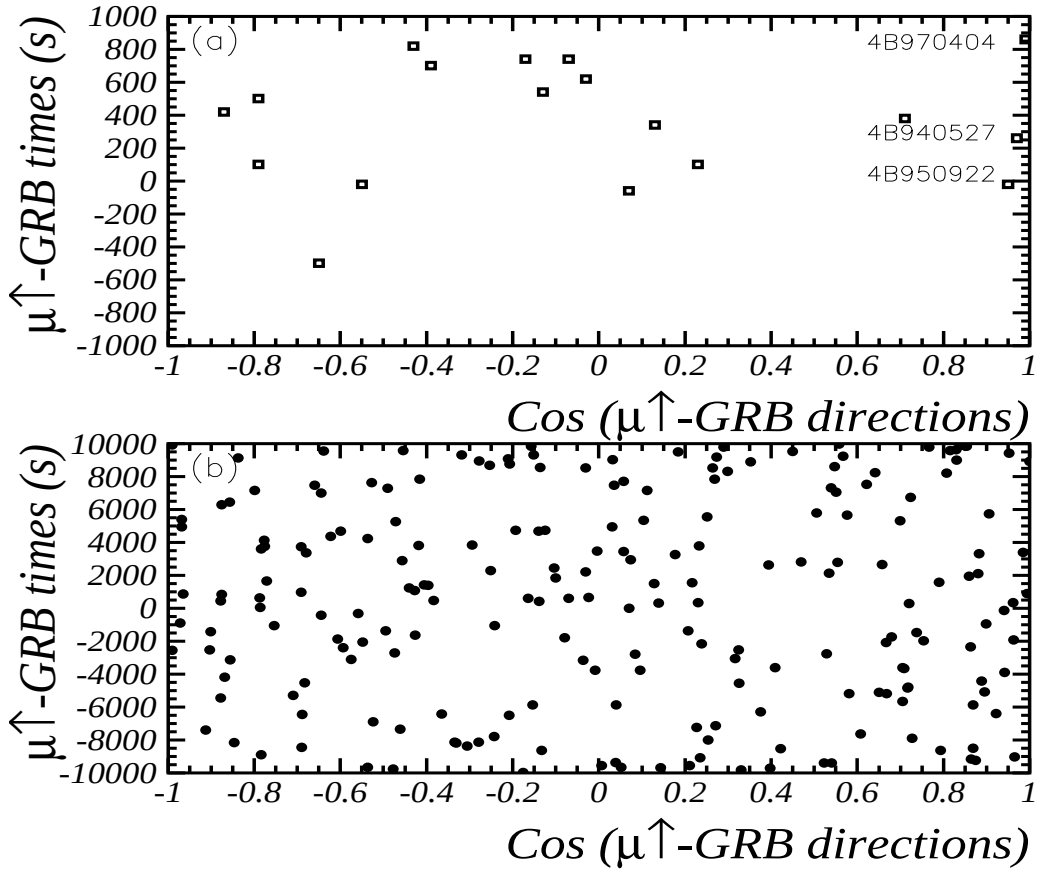

Fig. 15.— Difference in detection times vs the cosine of the angular separation between MACRO upward-going muon events and BATSE gamma ray bursts. (a) and (b) have different time scales. The BATSE GRB of 22 Sep. 1995 (4B 950922) was detected 39.4 s before one MACRO event at an angular distance of 17.6° and the BATSE (4B 940527) GRB of 27 May 1994 after 280 s another very horizontal MACRO event at 14.9°. In (a) they are indicated with the name of the bursts.

Table 6: Upper limits (90%c.l.) on upward muon fluxes induced by neutrinos from annihilation of neutralinos trapped in the Galactic Center for neutralino masses $m_\chi = 60$, 100, 200, 500 GeV and various search cones around its direction. These limits are for $E_\mu > 1$ GeV and upper limits are calculated according to (69). These limits constrain strongly the model by Gondolo and Silk (22) (compare them to Fig. 3 in their paper.)

Cone	Data	Background	m_χ (GeV)				
			60	100	200	500	1000
			μ-Flux limits $\times 10^{-15}$ cm^{-2}s^{-1}				
3°	0	0.9	3.67	3.42	3.26	3.21	3.21
5°	1	2.6	4.70	4.37	4.17	4.11	4.11
10°	10	10.3	13.66	12.71	12.11	11.96	11.94